

## Triphenylphosphane-Modified Cobalt Catalysts for the Selective Carbonylation of Ethyl Diazoacetate

Neszta Ungvári,<sup>†</sup> Eszter Fördös,<sup>†</sup> János Balogh,<sup>†</sup> Tamás Kégl,<sup>†</sup> László Párkányi,<sup>‡</sup> and Ferenc Ungváry<sup>\*,†</sup><sup>†</sup>Department of Organic Chemistry, University of Pannonia, 8201 Veszprém, Egyetem u. 10, Hungary, and <sup>‡</sup>Institute of Structural Chemistry, Chemical Research Center, Hungarian Academy of Sciences, P.O. Box 17, 1525 Budapest, Hungary

Received May 17, 2010

The triphenylphosphane-substituted carbonyl cobalt complexes  $\text{Co}_2(\text{CO})_7(\text{PPh}_3)$ ,  $\text{Co}_2(\text{CO})_6(\text{CHCO}_2\text{Et})(\text{PPh}_3)$ , and  $[\text{Co}(\text{CO})_3(\text{PPh}_3)_2][\text{Co}(\text{CO})_4]$  were found to be more effective precatalysts in the carbonylation of ethyl diazoacetate under atmospheric pressure of carbon monoxide at 10 °C in dichloromethane solution than the parent  $\text{Co}_2(\text{CO})_8$  and  $\text{Co}_2(\text{CO})_7(\text{CHCO}_2\text{Et})$  complexes. The highly reactive (ethoxycarbonyl)ketene is the primary product of the catalytic carbonylation, which dimerizes in the absence of a proper scavenger. In the presence of ethanol as the trapping reagent diethyl malonate is the final product of the carbonylation reaction. The formation of (ethoxycarbonyl)ketene using the catalyst precursor  $\text{Co}_2(\text{CO})_7(\text{PPh}_3)$  occurs in a catalytic cycle, where  $\text{Co}_2(\text{CO})_6(\text{PPh}_3)$  and  $\text{Co}_2(\text{CO})_6(\text{CHCO}_2\text{Et})(\text{PPh}_3)$  are the repeating species. The 16e species  $\text{Co}_2(\text{CO})_6(\text{PPh}_3)$  is involved in the deazotization of ethyl diazoacetate, and  $\text{Co}_2(\text{CO})_6(\text{CHCO}_2\text{Et})(\text{PPh}_3)$  leads to the (ethoxycarbonyl)ketene formation. In the absence of carbon monoxide or at low CO concentration the reaction of  $\text{Co}_2(\text{CO})_6(\text{CHCO}_2\text{Et})(\text{PPh}_3)$  with ethyl diazoacetate is the source of  $\text{Co}_2(\text{CO})_5(\text{CHCO}_2\text{Et})_2(\text{PPh}_3)$ , which is not an active catalyst for the carbonylation of ethyl diazoacetate. Using  $[\text{Co}(\text{CO})_3(\text{PPh}_3)_2][\text{Co}(\text{CO})_4]$  as the catalyst precursor, the intermediary formation of  $[\text{Co}(\text{CO})_3(\text{PPh}_3)_2][\text{Co}(\text{CO})_3(\text{O}=\text{C}=\text{CHCO}_2\text{Et})]$  through radical pairs is assumed. Substituting  $\text{PPh}_3$  in  $\text{Co}_2(\text{CO})_7(\text{PPh}_3)$ ,  $\text{Co}_2(\text{CO})_6(\text{CHCO}_2\text{Et})(\text{PPh}_3)$ , and  $[\text{Co}(\text{CO})_3(\text{PPh}_3)_2][\text{Co}(\text{CO})_4]$  by polymer-bound  $\text{PPh}_3$  results in active and reusable catalysts for the selective carbonylation of ethyl diazoacetate in dichloromethane solution at 40 °C and 11 bar of pressure with up to 5.1 mol of product/(mol of catalyst h) turnover frequency.

## 1. Introduction

The substitution of the diazo group in diazoalkanes by carbon monoxide to obtain ketenes has great potential in synthetic organic chemistry.<sup>1,2</sup> Among the various transition-metal complexes capable of mediating the ketene formation,<sup>3</sup>  $\text{Co}_2(\text{CO})_8$  was found to be a highly active and selective catalyst for the preparation of (trimethylsilyl)ketene by the carbonylation of (trimethylsilyl)diazomethane.<sup>4</sup> The very reactive (ethoxycarbonyl)ketene formed in the  $\text{Co}_2(\text{CO})_8$ -catalyzed carbonylation of ethyl diazoacetate can be trapped in situ by alcohols, phenol, secondary amines, or imines to obtain the corresponding malonic acid derivatives<sup>3,5</sup> or  $\beta$ -lactams,<sup>6</sup> respectively, in high yields

using simple one-pot procedures. The mechanism of the catalytic carbonylation of ethyl diazoacetate in  $\text{CH}_2\text{Cl}_2$  solution at 10 °C in the presence of ethanol using  $\text{Co}_2(\text{CO})_8$  as the catalyst precursor has been established. According to Scheme 1 the formation of diethyl malonate occurs in parallel in two different cycles, **A** and **B**. In the first cycle  $\text{Co}_2(\text{CO})_7$  and  $\text{Co}_2(\text{CO})_7(\text{CHCO}_2\text{Et})$  are the working repeating species, whereas in the second cycle the species are  $\text{Co}_2(\text{CO})_6(\text{CHCO}_2\text{Et})$  and  $\text{Co}_2(\text{CO})_6(\text{CHCO}_2\text{Et})_2$ . On the basis of the experimentally determined rates of the steps in the suggested cycles and the composition of the cobalt complexes in the reaction mixture under various conditions, the contribution of cycles **A** and **B** to the formation of the diethyl malonate product were calculated. According to the calculations most of the diethyl malonate product forms in cycle **B** at low (1 bar) carbon monoxide pressure, but in cycle **A** formation occurs if the carbon monoxide pressure is high (100 bar).<sup>7</sup>

We found that triphenylphosphane-substituted cobalt carbonyl complexes such as  $\text{Co}_2(\text{CO})_7(\text{PPh}_3)$ <sup>8–10</sup> (**1**),  $\text{Co}_2(\text{CO})_6(\text{PPh}_3)_2$ <sup>11</sup> (**2**),  $\text{Co}_2(\text{CO})_6(\text{CHCO}_2\text{Et})(\text{PPh}_3)$ <sup>12</sup> (**3**),

\*To whom correspondence should be addressed. E-mail: ungvary@almos.vein.hu.

(1) Tidwell, T. T. *Ketenes*, 2nd ed.; Wiley: Hoboken, NJ, 2006.

(2) Tidwell, T. T. *Eur. J. Org. Chem.* **2006**, 563–576.

(3) Ungvári, N.; Ungváry, F. Carbonylation of diazoalkanes. In *Modern Carbonylation Methods*; Kollár, L., Ed.; Wiley-VCH: Weinheim, Germany, 2008; Chapter 8, pp 199–221.

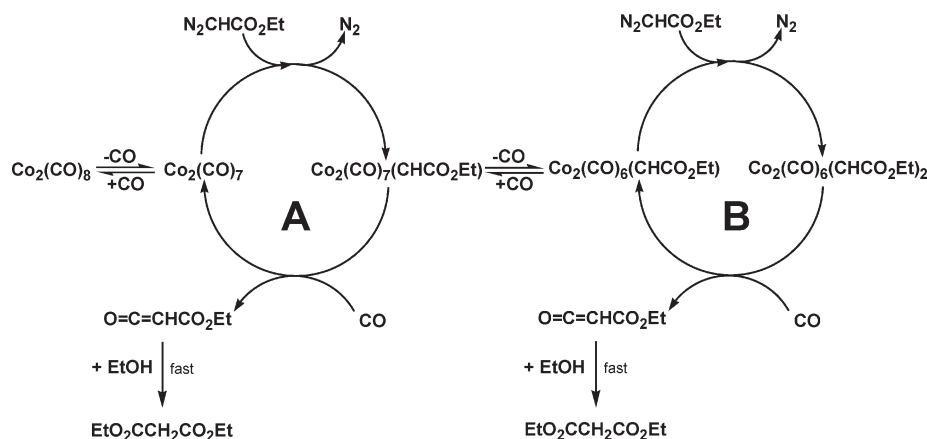
(4) Ungvári, N.; Kégl, T.; Ungváry, F. *J. Mol. Catal. A: Chem.* **2004**, 219, 7–11.

(5) Tuba, R.; Ungváry, F. *J. Mol. Catal. A: Chem.* **2003**, 203, 59–67.

(6) Fördös, E.; Tuba, R.; Párkányi, L.; Kégl, T.; Ungváry, F. *Eur. J. Org. Chem.* **2009**, 1994–2002.

(7) Ungvári, N.; Fördös, E.; Kégl, T.; Ungváry, F. *Inorg. Chim. Acta* **2010**, 363, 2016–2028.

(8) Bor, G.; Markó, L. *Chem. Ind.* **1963**, 912–913.

**Scheme 1. Mechanism of the Catalytic Carbonylation of Ethyl Diazoacetate in the Presence of Ethanol using  $\text{Co}_2(\text{CO})_8$  as the Catalyst Precursor**

$\text{Co}_2(\text{CO})_5(\text{CHCO}_2\text{Et})(\text{PPh}_3)_2$  (**4**), and  $[\text{Co}(\text{CO})_3(\text{PPh}_3)_2][\text{Co}(\text{CO})_4]^{11,13}$  (**5**) are all useful precursors for the catalytic carbonylation of ethyl diazoacetate. Thus, using 2 mol % of these complexes under 50 bar pressure of carbon monoxide at 45 °C in the presence of ethanol, up to 100% yield of diethyl malonate was achieved in 24–150 h reaction time.<sup>12</sup> With the exception of **2** and **4** these complexes are active at lower temperature (10 °C) and under atmospheric pressure of carbon monoxide as well. Under the milder conditions they show even higher catalytic activity than  $\text{Co}_2(\text{CO})_8$  in the carbonylation of ethyl diazoacetate. On the basis of the results of infrared spectroscopic, preparative, and kinetic studies a tentative mechanism of these catalytic reactions is now reported.

Catalytic carbonylation of ethyl diazoacetate in dichloromethane solution using the immobilized analogues of **5**,<sup>10,14,15</sup> **1**,<sup>10,14,15</sup> and **3** on polymer-bound triphenylphosphane as the catalysts give at 40 °C and 11 bar of CO pressure products close to 100% yields free of cobalt with up to 5.1 mol/(mol h) turnover frequency.

## 2. Experimental Section

**2.1. General Procedures.** Handling of the cobalt carbonyl complexes was carried out under an atmosphere of dry  $\text{P}_4\text{O}_{10}$  and deoxygenated (BTS contact, room temperature) argon or carbon monoxide utilizing standard Schlenk techniques.<sup>16</sup> Dichloromethane was dried and distilled under an atmosphere of argon or carbon monoxide according to standard procedures.<sup>17</sup> IR spectra were recorded on Thermo Nicolet Avatar 330 and Bruker Tensor 27 FTIR spectrometers using 0.002 65, 0.007 65, 0.0218, or 0.0505 cm  $\text{CaF}_2$  liquid cells, calibrated by

the interference method.<sup>18</sup>  $^1\text{H}$ ,  $^{13}\text{C}$ , and  $^{31}\text{P}$  NMR spectra were recorded at room temperature on a Bruker 400 MHz spectrometer using  $\text{CDCl}_3$  as the solvent for solution spectra. Cobalt and phosphorus analyses were carried out by using an ICP-OES apparatus (inductively coupled plasma optical emission spectrometer from Perkin-Elmer) from samples prepared with concentrated nitric acid by using the HPA-S apparatus (high-pressure asher from Anton-Paar, Graz, Austria). Heptacarbonyl(triphenylphosphane)dicobalt(0),<sup>10</sup> octacarbonyldicobalt,<sup>19</sup> the  $\mu_2$ -(ethoxycarbonyl)carbene complexes **3**<sup>12</sup> and **4**,<sup>12</sup>  $[\text{Co}(\text{CO})_3(\text{PPh}_3)_2][\text{Co}(\text{CO})_4]^{11,13}$  (IR:  $\epsilon_{\text{M}}^{2010\text{ cm}^{-1}} = 3556$ , and  $\epsilon_{\text{M}}^{1890\text{ cm}^{-1}} = 5752$   $\text{cm}^2/\text{mmol}$  in  $\text{CH}_2\text{Cl}_2$ ),  $\text{Na}[\text{Co}(\text{CO})_4]^{20,21}$  (IR:  $\epsilon_{\text{M}}^{1887\text{ cm}^{-1}} = 335$ ,  $\epsilon_{\text{M}}^{1887\text{ cm}^{-1}} = 2995$ , and  $\epsilon_{\text{M}}^{1858\text{ cm}^{-1}} = 1366$   $\text{cm}^2/\text{mmol}$  in THF), and  $[\text{PPN}][\text{Co}(\text{CO})_4]^{22}$  ( $\text{PPN} = [\text{Ph}_3\text{P}=\text{N}=\text{PPh}_3]^+$ ) (IR:  $\epsilon_{\text{M}}^{1889\text{ cm}^{-1}} = 6100$   $\text{cm}^2/\text{mmol}$  in  $\text{CH}_2\text{Cl}_2$ ) were prepared by standard literature procedures. Stock solutions (0.050 mol/dm<sup>3</sup>) of  $[\text{Co}(\text{EtOH})_6][\text{Co}(\text{CO})_4]_2$  were prepared by dissolving  $\text{Co}_2(\text{CO})_8$  (257 mg, 0.75 mmol) in absolute EtOH (9.9  $\text{cm}^3$ ) under argon at room temperature (IR:  $\epsilon_{\text{M}}^{2010\text{ cm}^{-1}} = 140$ ,  $\epsilon_{\text{M}}^{1903\text{ cm}^{-1}} = 4230$   $\text{cm}^2/\text{mmol}$ , and a strong shoulder at  $1870\text{ cm}^{-1}$  in EtOH) and were used immediately after preparation. Carbon monoxide (99.99% purity) was obtained from Messer Hungary.  $^{13}\text{CO}$  (99% isotope purity) was obtained from Sigma-Aldrich. Cobaltocene (99% purity) was obtained from Strem. Polystyrenediphenylphosphane cross-linked with 1% divinylbenzene (1.6 mmol P/g, 100–200 mesh particle size) was obtained from Fluka, and polystyrenediphenylphosphane cross-linked with 1% divinylbenzene (~2.0 mmol P/g, 100–200 mesh particle size) was obtained from Sigma-Aldrich.

**2.2. Catalytic Carbonylations.** The catalytic carbonylation reactions of ethyl diazoacetate using soluble catalyst precursors were performed in a thermostated glass reactor at atmospheric pressure or in a glass insert of a thermostated autoclave at higher carbon monoxide pressure using 0.02–0.20 mmol aliquots of the catalyst precursor complexes in the form of freshly prepared stock solutions. The reactions were started by adding neat ethyl diazoacetate to the reaction mixture. The concentration of the carbonylation products and that of other components in the reaction mixture was determined at different time intervals from withdrawn samples by quantitative infrared spectroscopy. Initial rates of diethyl malonate formation were calculated from the concentrations determined using the molar absorptivities of diethyl malonate in  $\text{CH}_2\text{Cl}_2$  at  $1730$  and  $1749\text{ cm}^{-1}$  ( $\epsilon_{\text{M}}^{1730\text{ cm}^{-1}} = 666$   $\text{cm}^2/\text{mmol}$ ,  $\epsilon_{\text{M}}^{1749\text{ cm}^{-1}} = 579$   $\text{cm}^2/\text{mmol}$ ) between 5 and 15% conversions.

(9) Szabó, P.; Fekete, L.; Bor, G.; Nagy-Magos, Z.; Markó, L. *J. Organomet. Chem.* **1968**, *12*, 245–248.

(10) Comely, A. C.; Gibson, S. E.; Hales, N. J.; Johnstone, C.; Stevenazzi, A. *Org. Biomol. Chem.* **2003**, *1*, 1959–1968.

(11) Hieber, W.; Freyer, W. *Chem. Ber.* **1958**, *91*, 1230–1234.

(12) Tuba, R.; Fördös, E.; Ungvári, F. *J. Mol. Catal. A: Chem.* **2005**, *236*, 113–118.

(13) Vohler, O. *Chem. Ber.* **1958**, *91*, 1235–1238.

(14) Comely, A. C.; Gibson (née Thomas), S. E.; Hales, N. J. *Chem. Commun.* **1999**, 2075–2076.

(15) Comely, A. C.; Gibson (née Thomas), S. E.; Hales, N. J. *Chem. Commun.* **2000**, 305–306.

(16) Shriver, D. F. *The Manipulation of Air-Sensitive Compounds*; Krieger: Malabar, FL, 1982.

(17) Armarego, W. L. F.; Perrin, D. D. *Purification of Laboratory Chemicals*, 4th ed.; Butterworth-Heinemann: Oxford, U.K., 1996.

(18) Willard, H. H.; Merritt, L. L., Jr.; Dean, J. A.; Settle, F. A., Jr. *Instrumental Methods of Analysis*, 6th ed.; Wadsworth: Belmont, CA, 1981; p 206.

(19) Szabó, P.; Markó, L.; Bor, G. *Chem. Technol. (Leipzig)* **1961**, *13*, 549–550.

(20) Edgell, W. F.; Lyford, J., IV *Inorg. Chem.* **1970**, *9*, 1932–1933.

(21) Winzenburg, M. L. Ph.D. Thesis, University of Minnesota, 1979; Appendix A, p 152.

(22) Ruff, J. K.; Schlien, W. J. *Inorg. Synth.* **1974**, *15*, 84–90.

The catalytic carbonylation reactions of ethyl diazoacetate with the heterogenized catalysts were performed in a glass insert of a thermostated magnetically stirred autoclave between 5 and 50 bar of carbon monoxide pressure using 0.050 mmol portions of the catalysts. Recycling experiments were performed using a glass insert with a sintered glass frit (P3) which was closed on the bottom of the frit by a Teflon stopper. After the reaction the liquid product was removed from the glass insert under argon by filtration through the frit. When the bottom of the filter tube was closed by a Teflon stopper, new solvent and reactant were added to the recycled catalyst and a new cycle was started by pressurizing with CO.

**2.3. Photochemical Reactions.** Photochemical experiments were performed in a double-jacketed thermostated glass reactor using a Pen-Ray light source emitting at 254 or 366 nm (Ultraviolet Products Inc.) immersed into the reaction mixture in a protecting quartz tube.

**2.4. Synthesis of  $\text{Co}_2(\text{CO})_5(\text{CHCO}_2\text{Et})_2(\text{PPh}_3)$  (6).** To a solution of  $\text{Co}_2(\text{CO})_6(\text{CHCO}_2\text{Et})(\text{PPh}_3)$  (635 mg, 1.0 mmol) in dichloromethane (9.4 cm<sup>3</sup>) was added ethyl diazoacetate (0.106 cm<sup>3</sup>, 1.0 mmol) at 0 °C under argon. For 2 h argon was slowly bubbled through the reaction mixture, and then a second portion of ethyl diazoacetate (0.106 cm<sup>3</sup>, 1.0 mmol) was added, and the argon purging was continued for another 3 h period. After the reaction mixture was kept at 0 °C in the refrigerator overnight, the solution was filtered and concentrated to a volume of 3 cm<sup>3</sup> before flash column chromatography on silica gel (1.5 cm × 24 cm column) with dichloromethane as the eluent. The first 180 cm<sup>3</sup> fraction was discarded, and from the second 410 cm<sup>3</sup> fraction the solvent was removed under vacuum. Complex 6 was obtained as an orange oil (215 mg, 31% yield). TLC on silica gel/ $\text{CH}_2\text{Cl}_2$  gave one spot with  $R_f = 0.32$ . IR ( $\text{CH}_2\text{Cl}_2$ ): 2087 ( $\epsilon_M^{2087\text{ cm}^{-1}} = 522\text{ cm}^2/\text{mmol}$ ), 2041 ( $\epsilon_M^{2041\text{ cm}^{-1}} = 673\text{ cm}^2/\text{mmol}$ ), 1975 ( $\epsilon_M^{1975\text{ cm}^{-1}} = 3009\text{ cm}^2/\text{mmol}$ ), 1723 ( $\epsilon_M^{1723\text{ cm}^{-1}} = 121\text{ cm}^2/\text{mmol}$ ), 1685 ( $\epsilon_M^{1685\text{ cm}^{-1}} = 440\text{ cm}^2/\text{mmol}$ ) cm<sup>-1</sup>. <sup>1</sup>H NMR ( $\text{CDCl}_3$ ,  $\delta$ /ppm): 7.58–7.37 (m, 15 H,  $\text{C}_6\text{H}_5$ ), 4.15–3.29 (m, 4H,  $\text{CH}_2$ ), 2.13 (s, 2H, CH), 1.11 (m, 6H,  $\text{CH}_3$ ). <sup>13</sup>C NMR ( $\text{CDCl}_3$ ,  $\delta$ /ppm): 198.8 and 198.6 (term COs), 181.1 and 180.3 ( $\text{CO}_2\text{Et}$ ), 134.4–128.0 ( $\text{C}_6\text{H}_5$ ), 112.3 (CH), 60.5 and 59.5 ( $\text{CH}_2$ ), 14.1 ( $\text{CH}_3$ ) 5.2 (d,  $J_{\text{CP}} = 16\text{ Hz}$ , CH). <sup>31</sup>P NMR ( $\text{CDCl}_3$ ,  $\delta$ /ppm): 60.36.

**2.5. Synthesis of  $\text{EtO}_2\text{CCH}_2\text{Co}(\text{CO})_3(\text{PPh}_3)$ .** A solution of  $\text{Co}_2(\text{CO})_5(\text{CHCO}_2\text{Et})(\text{PPh}_3)_2$  (434 mg, 0.5 mmol) in dichloromethane (4.7 cm<sup>3</sup>) was refluxed under argon for 15 min. The brown precipitate (200 mg, 46 m/m%) was separated by filtration and washed with dichloromethane (3 × 2 cm<sup>3</sup>). IR (KBr): 1960 sh, 1943 vs, 1930 sh cm<sup>-1</sup>. IR ( $\text{CH}_2\text{Cl}_2$ ): 1969.6 m, 1941 vs, br, 1897 m cm<sup>-1</sup>. Flash column chromatography of the concentrated orange-red filtrate was performed on silica gel (1.0 cm × 24 cm column) with  $\text{CH}_2\text{Cl}_2$  as the eluent. The first 60 cm<sup>3</sup> fraction was discarded, and from the second 75 cm<sup>3</sup> fraction the solvent was removed under vacuum. The complex  $\text{EtO}_2\text{CCH}_2\text{Co}(\text{CO})_3(\text{PPh}_3)$  was obtained as yellow crystals (196 mg, 77% yield). IR ( $\text{CH}_2\text{Cl}_2$ ): 2046 ( $\epsilon_M^{2046\text{ cm}^{-1}} = 185\text{ cm}^2/\text{mmol}$ ), 1974 ( $\epsilon_M^{1974\text{ cm}^{-1}} = 2500\text{ cm}^2/\text{mmol}$ ), and 1685 ( $\epsilon_M^{1685\text{ cm}^{-1}} = 342\text{ cm}^2/\text{mmol}$ ) cm<sup>-1</sup>.

**2.6. Preparation of Polystyrenediphenylphosphane (PSDP)-Anchored Carbonyl Cobalt Catalyst from PSDP and  $\text{Co}_2(\text{CO})_8$ .** To polystyrenediphenylphosphane (2.32 g, 3.712 mmol P) in a filter tube (P3 frit 2.0 cm diameter, 31 cm<sup>3</sup> volume, fitted with a gas inlet for CO and a silicon septum and connected to a graduated Schlenk flask receiver of 100 cm<sup>3</sup> capacity) under a CO atmosphere was added dichloromethane (16 cm<sup>3</sup>) at room temperature. A slight positive pressure difference between the Schlenk flask and the filter (5–10 mmHg) kept the solvent in the filter tube and served to stir the mixture. After 30 min, a solution of  $\text{Co}_2(\text{CO})_8$  (0.762 g, 2.228 mmol) in dichloromethane (8.0 cm<sup>3</sup>) was added by a syringe. When the pressure difference was reversed after 60 min, the solution was collected in the Schlenk flask and the dark brown polymer beads were washed five times with 8 cm<sup>3</sup> portions of dichloromethane. The combined

dichloromethane solutions in the Schlenk flask contained 0.149 mmol of  $\text{Co}_2(\text{CO})_8$  (according to quantitative infrared analysis) not taken up by the polymer in the loading procedure. Drying the cobalt-loaded polymer first in a stream of CO and then under vacuum afforded 3.12 g of dark yellow-red beads as the final product. Anal. Calcd (for a composition of 88% of polymer-bound 5-type complex and 12% of polymer-bound 1-type complex): Co, 7.86; P, 3.69. Found: Co, 7.9; P, 3.7. IR (KBr):  $\nu(\text{CO})$  2072 m, 1992 vs, br, 1880 vs, br cm<sup>-1</sup>. <sup>31</sup>P NMR (solid state,  $\delta$ ): 65.0 ppm.

**2.7. Preparation of Polystyrenediphenylphosphane (PSDP)-Anchored Carbonyl Cobalt Catalyst from PSDP and  $\text{Co}_2(\text{CO})_7(\text{CHCO}_2\text{Et})$ .** Following the loading procedure as in part 2.6 but using a solution of  $\text{Co}_2(\text{CO})_7(\text{CHCO}_2\text{Et})$  (3.712 mmol) in dichloromethane (38 cm<sup>3</sup>) added in four installments to the dichloromethane-swelled polystyrenediphenylphosphane (2.32 g, 3.712 mmol P) resulted in 3.81 g of dark purple-red beads after drying. Anal. Calcd (for a polymer-bound 3-type complex): Co, 11.84; P, 3.11. Found: Co, 12.1; P, 3.0. IR (KBr):  $\nu(\text{CO})$  2075 m, 2029 s, 2011 s, 1997 m, br, 1975 m, br cm<sup>-1</sup> (complex 3 IR (KBr):  $\nu(\text{CO})$  2075 s, 2027 s, 2017 s, 2005 s, 1990 m, 1825 s, 1668 m cm<sup>-1</sup>). <sup>31</sup>P NMR (solid state,  $\delta$ ): 61.0 ppm.

**2.8. Preparation of Polystyrenediphenylphosphane (PSDP)-Anchored  $\text{N}_2\text{CHCO}_2\text{Et}$ .** Using in the loading procedure polystyrenediphenylphosphane (1.03 g, 2.047 mmol P) and ethyl diazoacetate (0.37 g, 3.24 mmol) gave recovered ethyl diazoacetate in the filtrate (0.14 g, 1.23 mmol), and 1.26 g of yellow beads in the filter tube after drying. Anal. Calcd (for a polymer-bound  $\text{Ph}_3\text{P}=\text{NN}=\text{CHCO}_2\text{Et}$ -type phosphazane): P, 5.02. Found: P, 4.9. IR (KBr):  $\nu(\text{C}=\text{O})$  1710 s,  $\nu(\text{N}=\text{C})$  1675 s,  $\nu(\text{P}=\text{N})$  1520 cm<sup>-1</sup>. <sup>31</sup>P NMR ( $\text{CH}_2\text{Cl}_2$ -swelled beads,  $\delta$ ): 19.3 ppm.

**2.9. <sup>13</sup>CO Exchange Reactions.** The <sup>13</sup>CO exchange reactions of  $[\text{Co}(\text{CO})_3(\text{PPh}_3)_2][\text{Co}(\text{CO})_4]$  (5),  $[\text{Co}(\text{EtOH})_6][\text{Co}(\text{CO})_4]_2$  (7),  $\text{Na}[\text{Co}(\text{CO})_4]$  (8), and  $[\text{PPN}][\text{Co}(\text{CO})_4]$  (9) were performed with 0.03–0.05 mmol amounts of the complexes and 1.0 mmol of <sup>13</sup>CO in a thermostated glass reactor at atmospheric pressure. The change in the concentration of the complexes was followed by quantitative infrared spectroscopy using a syringe pump to circulate the reaction mixture between the reactor and the infrared liquid cell.

**2.10. Theoretical Methods.** All of the minima and transition states were computed with the hybrid HF/DFT method using the combination of the three-parameter Becke exchange functional with the Lee–Yang–Parr correlation functional known as B3LYP.<sup>23</sup> For cobalt atoms the Stevens–Basch–Krauss–Jasien–Cundari basis set, which is valence triple- $\zeta$  for transition metals, with the corresponding small-core pseudopotential<sup>24</sup> was utilized. This basis set follows the contraction pattern of (8s,8p,6d) → [4s,4p,3d] for cobalt. For the other atoms the 6-31G(d,p) basis set<sup>25</sup> was used.

The calculations were carried out using PC-GAMESS 7.1.E/Firefly software,<sup>26</sup> which is partially based on the GAMESS-US source code<sup>27</sup> and the Gaussian 03 suite of programs.<sup>28</sup> Local minima were identified by the absence of negative eigenvalues in the vibrational frequency analysis. The Hessian matrix of transition state structures has only one negative eigenvalue. Intrinsic reaction coordinate (IRC) analyses<sup>29</sup> were used at the same level of theory as the geometry optimizations in order to confirm that the stationary points are smoothly connected to each other. To estimate the effect of the solvent, single-point

(23) Becke, A. D. *J. Chem. Phys.* **1993**, *98*, 5648–5652.

(24) Stevens, W. J.; Basch, H.; Krauss, M. *J. Chem. Phys.* **1984**, *81*, 6026–6033.

(25) Hehre, W. J.; Ditchfield, R.; Pople, J. A. *J. Chem. Phys.* **1972**, *56*, 2257–2261.

(26) <http://classic.chem.msu.su/gran/games/index.html>.

(27) Schmidt, M. W.; Baldridge, K. K.; Boatz, J. A.; Elbert, S. T.; Gordon, M. S.; Jensen, J. H.; Koseki, S.; Matsunaga, N.; Nguyen, K. A.; Su, S.; Windus, T. L.; Dupuis, M.; Montgomery, J. A. *J. Comput. Chem.* **1993**, *14*, 1347–1363.



**Table 1.** Initial Rate of Diethyl Malonate Formation ( $r_{\text{DEM}}$ ) in the Carbonylation of Ethyl Diazoacetate (EDA) ( $[\text{EDA}]_0 = [\text{EtOH}]_0 = 0.25 \text{ mol/dm}^3$ ) at 10 °C in  $\text{CH}_2\text{Cl}_2$  Solution under Atmospheric Pressure of Carbon Monoxide ( $[\text{CO}]_0 = 0.00500\text{--}0.00510 \text{ mol/dm}^3$ ) in the Presence of Different Carbonyl Cobalt Complexes as the Precatalysts:  $\text{Co}_2(\text{CO})_8$ ,  $\text{Co}_2(\text{CO})_7(\text{PPh}_3)$  (**1**),  $\text{Co}_2(\text{CO})_6(\text{CHCO}_2\text{Et})(\text{PPh}_3)$  (**3**),  $\text{Co}_2(\text{CO})_5(\text{CHCO}_2\text{Et})(\text{PPh}_3)_2$  (**4**), and  $[\text{Co}(\text{CO})_3(\text{PPh}_3)_2][\text{Co}(\text{CO})_4]$  (**5**)

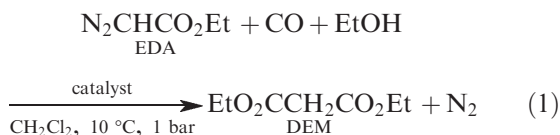
entry	$[\text{Co}_2(\text{CO})_8]_0$ (mol/dm <sup>3</sup> )	$[\text{1}]_0$ (mol/dm <sup>3</sup> )	$[\text{3}]_0$ (mol/dm <sup>3</sup> )	$[\text{4}]_0$ (mol/dm <sup>3</sup> )	$[\text{5}]_0$ (mol/dm <sup>3</sup> )	$[\text{PPh}_3]_0$ (mol/dm <sup>3</sup> )	$10^3 r_{\text{DEM}}$ (mol/(dm <sup>3</sup> s))
1	0.050						0.50
2		0.050					4.95
3		0.050					0.48 <sup>a</sup>
4			0.050				10.85
5			0.050				1.36 <sup>b</sup>
6				0.050			3.00
7				0.050			0.11
8					0.0050	0.500	3.30
9					0.0050		3.33 <sup>c</sup>
10					0.0050		3.28 <sup>d</sup>
11					0.0050		1.35 <sup>e</sup>
12					0.0050		0.67 <sup>f</sup>
13					0.0050	0.012	2.11
14					0.0050	0.025	1.55
15					0.0050	0.050	0.67
16					0.0050		0.17 <sup>g</sup>

<sup>a</sup> Under 3152 mmHg pressure of carbon monoxide,  $[\text{CO}]_0 = 0.0288 \text{ mol/dm}^3$ . <sup>b</sup> Under 1544 mmHg pressure of carbon monoxide,  $[\text{CO}]_0 = 0.01298 \text{ mol/dm}^3$ . <sup>c</sup>  $[\text{EtOH}]_0 = 0.50 \text{ mol/dm}^3$ . <sup>d</sup>  $[\text{EtOH}]_0 = 1.00 \text{ mol/dm}^3$ . <sup>e</sup>  $[\text{EDA}]_0 = 0.10 \text{ mol/dm}^3$ . <sup>f</sup>  $[\text{EDA}]_0 = 0.05 \text{ mol/dm}^3$ . <sup>g</sup> Under 10 bar pressure of carbon monoxide,  $[\text{CO}]_0 = 0.072 \text{ mol/dm}^3$ .

calculations on the gas-phase optimized structures were carried out employing the polarized continuum model (PCM)<sup>30</sup> with the dielectric constant  $\epsilon_0 = 8.93$  for dichloromethane.

### 3. Results

Typical initial rates of diethyl malonate formation ( $r_{\text{DEM}}$ ) in the carbonylation reaction of ethyl diazoacetate (EDA) according to eq 1 using different cobalt complexes as the catalyst precursors are compiled in Table 1.



The  $r_{\text{DEM}}$  data in Table 1 show that using the  $\text{PPh}_3$ -containing carbonyl cobalt complexes  $\text{Co}_2(\text{CO})_7(\text{PPh}_3)$  (**1**),  $\text{Co}_2(\text{CO})_6(\text{CHCO}_2\text{Et})(\text{PPh}_3)$  (**3**),  $\text{Co}_2(\text{CO})_5(\text{CHCO}_2\text{Et})(\text{PPh}_3)_2$  (**4**), and  $[\text{Co}(\text{CO})_3(\text{PPh}_3)_2][\text{Co}(\text{CO})_4]$  (**5**) as catalyst precursors result in more active catalysts than  $\text{Co}_2(\text{CO})_8$ .

Using  $\text{Co}_2(\text{CO})_7(\text{PPh}_3)$  (**1**) as the precatalyst, the initial rate of diethyl malonate formation ( $r_{\text{DEM}}$ ) (entry 2) is 10 times

higher than that observed with  $\text{Co}_2(\text{CO})_8$  (entry 1). In 3 h reaction time complete conversion of the starting ethyl diazoacetate (EDA) into diethyl malonate (DEM) occurs with complex **1** but only 20% conversion with  $\text{Co}_2(\text{CO})_8$ .<sup>7</sup> The infrared spectra of the reaction mixtures of the former show at different conversions the presence of complex **1** at 2078, 2023, 1988, 1955, and 1818  $\text{cm}^{-1}$  ( $\epsilon_{\text{M}}^{2078 \text{ cm}^{-1}} = 2381$ ,  $\epsilon_{\text{M}}^{2023 \text{ cm}^{-1}} = 1147$ ,  $\epsilon_{\text{M}}^{1988 \text{ cm}^{-1}} = 4205$ ,  $\epsilon_{\text{M}}^{1955 \text{ cm}^{-1}} = 609$ , and  $\epsilon_{\text{M}}^{1818 \text{ cm}^{-1}} = 90 \text{ cm}^2/\text{mmol}$  in  $\text{CH}_2\text{Cl}_2$ )<sup>31</sup> and a shoulder at 2033  $\text{cm}^{-1}$ , which is the most intense band of complex **3**.<sup>12</sup> When the CO pressure is raised from atmospheric to 4 bar, the initial rate of diethyl malonate formation ( $r_{\text{DEM}}$ ) is strongly reduced (entry 3), and the shoulder at 2033  $\text{cm}^{-1}$  cannot be seen in the infrared spectrum of the reaction mixture. According to the X-ray structure of the crystalline  $\text{Co}_2(\text{CO})_7(\text{PPh}_3)$  (see Figure S10 in the Supporting Information, CCDC 756129) there is no carbon monoxide ligand(s) in a bridging position. However, two of the equatorial carbonyl ligands around the cobalt atoms are tilted by 6–7° toward the neighboring cobalt atoms.

With complex **3** as the catalyst precursor (entry 4), 22 times higher initial rate of the carbonylation reaction of EDA was observed than with  $\text{Co}_2(\text{CO})_8$ . In 20 min 50% conversion and in 180 min practically complete conversion of EDA into DEM was observed. At 50% conversion the composition of the cobalt complexes in the solution is 90% complex **3** ( $\epsilon_{\text{M}}^{2080 \text{ cm}^{-1}} = 1517$ ,  $\epsilon_{\text{M}}^{2033 \text{ cm}^{-1}} = 2941$ ,  $\epsilon_{\text{M}}^{2013 \text{ cm}^{-1}} = 2462$ ,  $\epsilon_{\text{M}}^{1829 \text{ cm}^{-1}} = 597$ ,  $\epsilon_{\text{M}}^{1688 \text{ cm}^{-1}} = 174$ , and  $\epsilon_{\text{M}}^{1666 \text{ cm}^{-1}} = 151 \text{ cm}^2/\text{mmol}$  in  $\text{CH}_2\text{Cl}_2$ ) and 10% complex **1**, according to the infrared spectra of the reaction mixture. Raising the carbon monoxide pressure to 2 bar strongly inhibits the rate of diethyl malonate formation (entry 5). In experiments started under atmospheric pressure of carbon monoxide new bands grow in at 2087 and 2041  $\text{cm}^{-1}$  at higher conversions. If complex **3** and EDA are applied in a 1:1 to 1:2 molar ratio in the absence of carbon monoxide and ethanol, the complex with the characteristic absorptions at 2087 and 2041  $\text{cm}^{-1}$  becomes the main

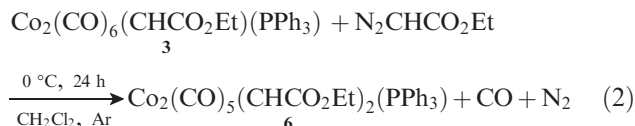
(28) Frisch, M. J.; Trucks, G. W.; Schlegel, H. B.; Scuseria, G. E.; Robb, M. A.; Cheeseman, J. R.; Montgomery, J. A., Jr.; Vreven, T.; Kudin, K. N.; Burant, J. C.; Millam, J. M.; Iyengar, S. S.; Tomasi, J.; Barone, V.; Mennucci, B.; Cossi, M.; Scalmani, G.; Rega, N.; Petersson, G. A.; Nakatsuji, H.; Hada, M.; Ehara, M.; Toyota, K.; Fukuda, R.; Hasegawa, J.; Ishida, M.; Nakajima, T.; Honda, Y.; Kitao, O.; Nakai, H.; Klene, M.; Li, X.; Knox, J. E.; Hratchian, H. P.; Cross, J. B.; Bakken, V.; Adamo, C.; Jaramillo, J.; Gomperts, R.; Stratmann, R. E.; Yazyev, O.; Austin, A. J.; Cammi, R.; Pomelli, C.; Ochterski, J. W.; Ayala, P. Y.; Morokuma, K.; Voth, G. A.; Salvador, P.; Dannenberg, J. J.; Zakrzewski, V. G.; Dapprich, S.; Daniels, A. D.; Strain, M. C.; Farkas, O.; Malick, D. K.; Rabuck, A. D.; Raghavachari, K.; Foresman, J. B.; Ortiz, J. V.; Cui, Q.; Baboul, A. G.; Clifford, S.; Cioslowski, J.; Stefanov, B. B.; Liu, G.; Liashenko, A.; Piskorz, P.; Komaromi, I.; Martin, R. L.; Fox, D. J.; Keith, T.; Al-Laham, M. A.; Peng, C. Y.; Nanayakkara, A.; Challacombe, M.; Gill, P. M. W.; Johnson, B.; Chen, W.; Wong, M. W.; Gonzalez, C.; Pople, J. A. *Gaussian 03*; Gaussian, Inc., Wallingford, CT, 2004.

(29) Gonzalez, C.; Schlegel, H. B. *J. Chem. Phys.* **1989**, *90*, 2154–2161.

(30) Miertus, S.; Scrocco, E.; Tomasi, J. *J. Chem. Phys.* **1981**, *55*, 117–129.

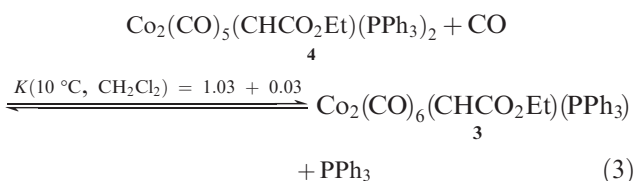
(31) In  $\text{CH}_2\text{Cl}_2$  solutions of  $\text{Co}_2(\text{CO})_7(\text{PPh}_3)$  a very weak absorption in the bridging  $\nu(\text{CO})$  range at 1818  $\text{cm}^{-1}$  is always present (see Figure S1 in the Supporting Information), which is, however, absent in hexane<sup>8,9</sup> or THF<sup>10</sup> solutions.

product of the reaction (eq 2). Flash column chromatography on silica gel with  $\text{CH}_2\text{Cl}_2$  at 4 °C affords the new complex in pure form as  $\text{Co}_2(\text{CO})_5(\text{CHCO}_2\text{Et})_2(\text{PPh}_3)$  (**6**) having absorptions in  $\text{CH}_2\text{Cl}_2$  solution at 2087 s, 2041 vs, 1979 vs, 1971 vs, 1723 w, and  $1685 \text{ m cm}^{-1}$ .



The carbonylation of ethyl diazoacetate with complex **6** as the precatalyst applied in  $0.005 \text{ mol/dm}^3$  concentration under the conditions shown in Table 1 results in  $<0.03 \text{ mol/(dm}^3 \text{ s)}$  initial rate of diethyl malonate formation.

Using complex **4** as the catalyst precursor, the initial rate of diethyl malonate formation (entry 6) was only about 28% of that observed with complex **3** (entry 4). In the infrared spectrum at 15% conversion of EDA the composition of the cobalt complexes in the solution is 30% of complex **3** and 70% of complex **4** on the basis of the intensity ratio of the bands at  $1829 \text{ cm}^{-1}$  ( $\epsilon_{\text{M}}^{1829 \text{ cm}^{-1}} = 597 \text{ cm}^2/\text{mmol}$ ) and  $1786 \text{ cm}^{-1}$  ( $\epsilon_{\text{M}}^{1786 \text{ cm}^{-1}} = 506 \text{ cm}^2/\text{mmol}$ ). When this experiment was repeated in the presence of a 10-fold molar excess of added  $\text{PPh}_3$  (entry 7), only trace amounts of complex **3** were formed from complex **4** and the initial rate of DEM formation dropped to about 4% of that without added  $\text{PPh}_3$  (entry 6). These results suggest that complex **3** rather than complex **4** is responsible for the catalytic DEM formation observed in entries 5 and 6, since these complexes are in equilibrium<sup>32</sup> according to eq 3. In addition the observed three bands in the infrared spectrum at 1711, 1688, and  $1534 \text{ cm}^{-1}$  revealed the formation of the known phosphazane  $\text{Ph}_3\text{P}=\text{NN}=\text{CHCO}_2\text{Et}$ <sup>33</sup> ( $\epsilon_{\text{M}}^{1711 \text{ cm}^{-1}} = 340$ ,  $\epsilon_{\text{M}}^{1688 \text{ cm}^{-1}} = 308$ , and  $\epsilon_{\text{M}}^{1534 \text{ cm}^{-1}} = 349 \text{ cm}^2/\text{mmol}$ ) from ethyl diazoacetate and the excess  $\text{PPh}_3$ .



If a solution of complex **4** in  $\text{CH}_2\text{Cl}_2$  without any other added reagents is refluxed under argon within a few minutes, it completely converts into a product which consists of a brown precipitate of the composition  $[\text{Co}(\text{CO})_2(\text{PPh}_3)]_x$  (46% m/m yield based on complex **4**; IR (KBr) 1960 sh, 1943 vs,  $1930 \text{ sh cm}^{-1}$ ; IR ( $\text{CH}_2\text{Cl}_2$ ) 1969.6 m, 1941 vs, br  $1897 \text{ m cm}^{-1}$ ) and an orange-red solution with the main characteristic IR band at  $1974 \text{ cm}^{-1}$ . Flash column chromatography on silica gel with  $\text{CH}_2\text{Cl}_2$  separates this component as yellow crystals in pure form as the known  $\text{EtO}_2\text{CCH}_2$ -

$\text{Co}(\text{CO})_3(\text{PPh}_3)^{34-36}$  in 77% isolated yield (based on the  $\text{CHCO}_2\text{Et}$  content of complex **4**) having absorptions in  $\text{CH}_2\text{Cl}_2$  solution at 2046 ( $\epsilon_{\text{M}}^{2046 \text{ cm}^{-1}} = 185 \text{ cm}^2/\text{mmol}$ ), 1974 ( $\epsilon_{\text{M}}^{1974 \text{ cm}^{-1}} = 2500 \text{ cm}^2/\text{mmol}$ ), and  $1685 \text{ cm}^{-1}$  ( $\epsilon_{\text{M}}^{1685 \text{ cm}^{-1}} = 342 \text{ cm}^2/\text{mmol}$ ). A single-crystal X-ray diffraction study of our yellow solid product confirmed the assumed structure (see Figure S11 in the Supporting Information, CCDC 756130), which is basically identical with that of  $\text{EtO}_2\text{CCH}_2\text{Co}(\text{CO})_3(\text{PPh}_3)$ . The only difference is that in our low-temperature ( $133(2) \text{ K}$ ) structure the ethyl group is not disordered. X-ray studies of close analogues of similar [(alkoxycarbonyl)methyl]cobalt type complexes have also been described.<sup>37</sup>

The complex  $[\text{Co}(\text{CO})_3(\text{PPh}_3)_2][\text{Co}(\text{CO})_4]$  (**5**) under an atmosphere of carbon monoxide shows a remarkable activity in the selective carbonylation of ethyl diazoacetate. Even at low concentrations ( $0.0050 \text{ mol/dm}^3$ ) complex **5** (entry 8) is more active than  $\text{Co}_2(\text{CO})_8$  (entry 1). Added  $\text{PPh}_3$  lowers the observed initial rate of carbonylation (entries 13–15). The initial rate of the carbonylation reaction is lower at 10 bar pressure of CO (entry 16) than under atmospheric pressure. The initial rate of diethyl malonate formation ( $r_{\text{DEM}}$ ) is first order in EDA and zero order in EtOH concentration (compare the rate in entry 8 with those in entries 9–12). The infrared spectra of the reaction mixtures containing the catalyst, EDA, and ethanol show bands at 2112, 2010, 1889, 1750, 1730, and  $1692 \text{ cm}^{-1}$  during the catalysis (see Figure 1 for an illustration). The  $\nu(\text{N}_2)$  and  $\nu(\text{CO})$  bands at 2112 and  $1692 \text{ cm}^{-1}$ , respectively, belong to the starting ethyl diazoacetate (EDA) ( $\epsilon_{\text{M}}^{2112 \text{ cm}^{-1}} = 800 \text{ cm}^2/\text{mmol}$  and  $\epsilon_{\text{M}}^{1692 \text{ cm}^{-1}} = 605 \text{ cm}^2/\text{mmol}$ ), the  $\nu(\text{CO})$  bands at 2010 and  $1889 \text{ cm}^{-1}$  ( $\epsilon_{\text{M}}^{2010 \text{ cm}^{-1}} = 3556 \text{ cm}^2/\text{mmol}$  and  $\epsilon_{\text{M}}^{1889 \text{ cm}^{-1}} = 5752 \text{ cm}^2/\text{mmol}$ ) belong to the catalyst complex  $[\text{Co}(\text{CO})_3(\text{PPh}_3)_2][\text{Co}(\text{CO})_4]$  (**5**), and the  $\nu(\text{CO})$  bands at 1750 and  $1730 \text{ cm}^{-1}$  belong to the product diethyl malonate (DEM) ( $\epsilon_{\text{M}}^{1750 \text{ cm}^{-1}} = 579 \text{ cm}^2/\text{mmol}$  and  $\epsilon_{\text{M}}^{1730 \text{ cm}^{-1}} = 666 \text{ cm}^2/\text{mmol}$ ). The intensity ratio of the bands at 2010 and  $1889 \text{ cm}^{-1}$  during the catalysis are, however, not the same as that in the spectrum of the original  $[\text{Co}(\text{CO})_3(\text{PPh}_3)_2][\text{Co}(\text{CO})_4]$  complex before participating in the carbonylation reaction. While the intensity of the band at  $2010 \text{ cm}^{-1}$  is unchanged during the catalytic carbonylation of ethyl diazoacetate, the band at  $1889 \text{ cm}^{-1}$  shows a small but significant decrease of intensity.

The change of the intensity ratio is much more pronounced in experiments started in the absence of ethanol (see Figure 2 for illustration). In Figure 2 we can see not only the dramatic decrease of the band intensity at  $1889 \text{ cm}^{-1}$  but the appearance of two new bands at 1734 and  $1637 \text{ cm}^{-1}$ . The band at  $1734 \text{ cm}^{-1}$  can be observed in the case of all the other cobalt catalysts as well if the carbonylation of ethyl diazoacetate is performed in the absence of ethanol, and this turned out to be the characteristic  $\nu(\text{C}=\text{O})$  band ( $\epsilon_{\text{M}}^{1734 \text{ cm}^{-1}} = 440 \text{ cm}^2/\text{mmol}$ ) of the known dimer of (ethoxycarbonyl)ketene, 3-(ethoxycarbonyl)-4-hydroxy-6-ethoxy-2H-pyran-2-one, which exists

(32) Ungvári, N.; Fördös, E.; Kégl, T.; Ungváry, F. *Inorg. Chim. Acta* **2009**, 362, 1333–1342.

(33) Staudinger, H.; Meyer, J. *Helv. Chim. Acta* **1919**, 2, 619–635.

(34) Galamb, V.; Pályi, G.; Cser, F.; Furmanova, M. G.; Struchkov, Y. T. *J. Organomet. Chem.* **1981**, 209, 183–195.

(35) Pályi, G.; Alberts, K.; Bartik, T.; Boese, R.; Fráter, G.; Herberich, T.; Herfurth, A.; Kriebel, C.; Sorkau, A.; Tschörner, C. M.; Zucchi, C. *Organometallics* **1996**, 15, 3253–3255.

(36) Bencze, L.; Szabó, M.; J. Szilágyi, R. K.; Boese, R.; Zucchi, C.; Pályi, G. In *Fundamentals of Life*; Pályi, G., Zucchi, C., Caglioti, L., Eds.; Elsevier: Paris, 2002; pp 451–471.

(37) (a) Szabó, M.; Szilágyi, R.; Bencze, L.; Boese, R.; Zucchi, C.; Caglioti, L.; Pályi, G. *Enantiomer* **2000**, 5, 549–559. (b) Zucchi, C.; Boese, R.; Alberts, K.; Herberich, T.; Tóth, G.; Bencze, L.; Pályi, G. *Eur. J. Inorg. Chem.* **2001**, 2297–2304. (c) Zucchi, C.; Tiddia, S.; Boese, R.; Tschörner, C. M.; Bencze, L.; Pályi, G. *Chirality* **2001**, 13, 458–464. (d) Zucchi, C.; Turini, D.; Boese, R.; Bencze, L.; Kurdi, R.; Caglioti, L.; Pályi, G. *Can. J. Chem.* **2005**, 83, 882–893.

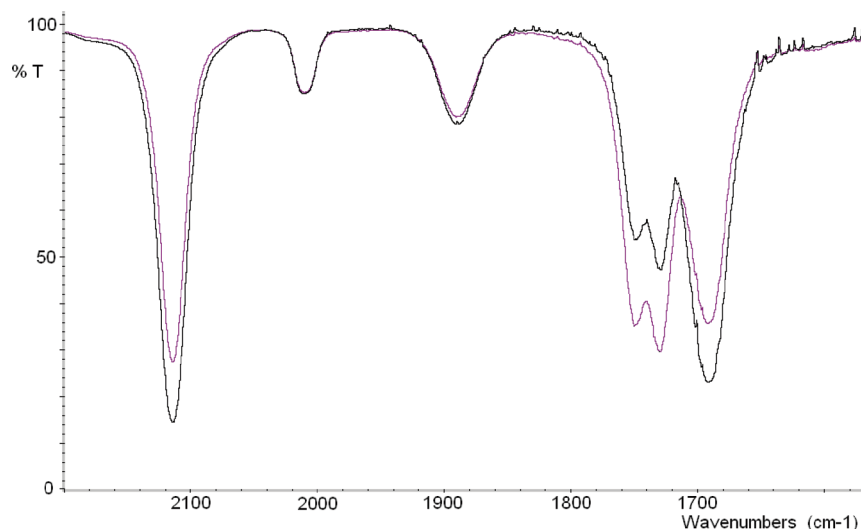


**Figure 1.** Change of the infrared spectra between 2200 and 1560  $\text{cm}^{-1}$  during the catalytic carbonylation of ethyl diazoacetate (EDA) in the presence of ethanol and  $[\text{Co}(\text{CO})_3(\text{PPh}_3)_2][\text{Co}(\text{CO})_4]$  (**5**) as the catalyst precursor under atmospheric pressure of carbon monoxide at 10  $^{\circ}\text{C}$  in  $\text{CH}_2\text{Cl}_2$  solution using a 0.007 65 cm  $\text{CaF}_2$  liquid cell: (black line) reaction time 30 min; (violet line) reaction time 90 min. Initial concentrations:  $[\text{EDA}]_0 = [\text{EtOH}]_0 = 0.25 \text{ mol/dm}^3$ ,  $[\mathbf{5}]_0 = 0.0050 \text{ mol/dm}^3$ ,  $[\text{CO}]_0 = 0.00506 \text{ mol/dm}^3$ .

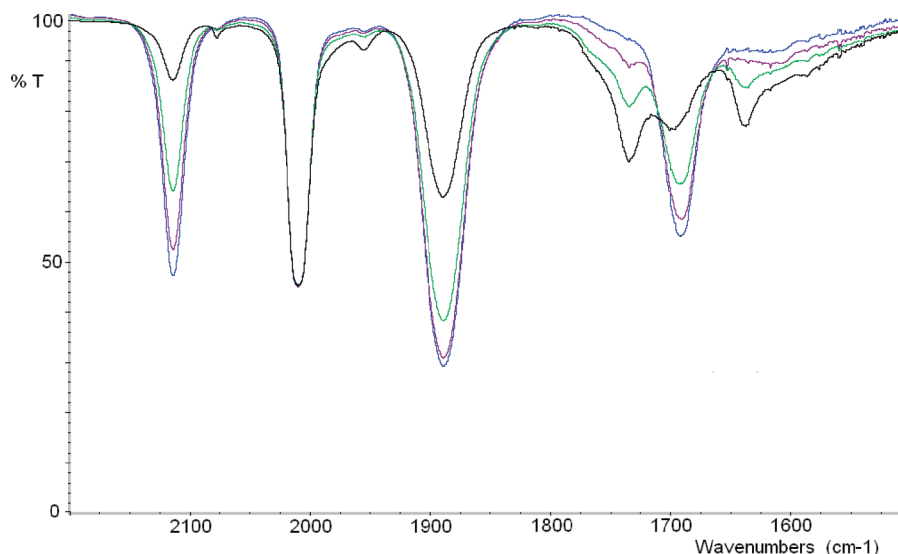
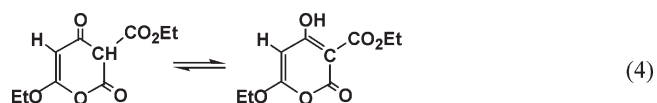


**Figure 2.** Change of the infrared spectra between 2200 and 1500  $\text{cm}^{-1}$  during the catalytic carbonylation of ethyl diazoacetate (EDA) in the absence of ethanol with  $[\text{Co}(\text{CO})_3(\text{PPh}_3)_2][\text{Co}(\text{CO})_4]$  (**5**) as the catalyst precursor under atmospheric pressure of carbon monoxide at 10  $^{\circ}\text{C}$  in  $\text{CH}_2\text{Cl}_2$  solution using a 0.021 80 cm  $\text{CaF}_2$  liquid cell: (blue line) reaction time 18 min; (violet line) reaction time 66 min; (green line) reaction time 134 min; (black line) reaction time 265 min. Initial concentrations:  $[\text{EDA}]_0 = 0.0182 \text{ mol/dm}^3$ ,  $[\mathbf{5}]_0 = 0.0045 \text{ mol/dm}^3$ ,  $[\text{CO}]_0 = 0.00504 \text{ mol/dm}^3$ .

as a solvent-dependent equilibrium mixture of the keto and enol forms (eq 4).<sup>38</sup>



The growing intensity of the band at 1637  $\text{cm}^{-1}$  and the declining intensity of the band at 1889  $\text{cm}^{-1}$  show a linear correlation (see Figure 5 in the Discussion).

In order to obtain reproducible initial rates, it was necessary to run the carbonylation experiments with the exclusion

of light. Especially  $[\text{Co}(\text{CO})_3(\text{PPh}_3)_2][\text{Co}(\text{CO})_4]$  (complex **5**) turned out to be extremely sensitive to light. Its electronic absorption spectrum in  $\text{CH}_2\text{Cl}_2$  shows an outer-sphere metal to metal charge transfer or intervalence transfer absorption band at 390 nm ( $\epsilon_{\text{M}}^{390 \text{ nm}} = 2645 \text{ cm}^2/\text{mmol}$ ). Irradiation of 0.005 M solutions of complex **5** in  $\text{CH}_2\text{Cl}_2$  at 366 nm results in rapid (< 1 min at 10  $^{\circ}\text{C}$ ) formation of  $\text{Co}_2(\text{CO})_6(\text{PPh}_3)_2$  (complex **2**) in the form of a sparingly soluble red-brown precipitate similar to that obtained in acetone solution.<sup>39</sup> If the irradiation was performed with a 1:1 molar mixture of  $\text{Co}_2(\text{CO})_8$  and  $[\text{Co}(\text{CO})_3(\text{PPh}_3)_2][\text{Co}(\text{CO})_4]$ , the rapid (< 1 min at 10  $^{\circ}\text{C}$ ) and quantitative formation of  $\text{Co}_2(\text{CO})_7(\text{PPh}_3)$  (complex **1**) was observed. Under thermal reaction

(38) Staudinger, H.; Becker, H. *Ber. Bunsen-Ges. Phys. Chem.* **1927**, 50, 1016–1024.

(39) Vogler, A.; Kunkely, H. *Organometallics* **1988**, 7, 1449–1450.

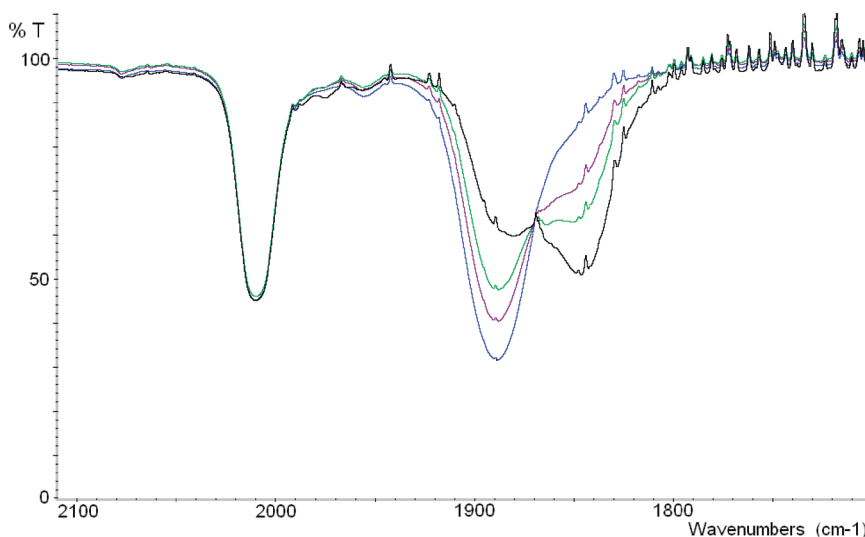


**Figure 3.** Change of the infrared spectra of  $[\text{Co}(\text{CO})_3(\text{PPh}_3)_2][\text{Co}(\text{CO})_4]$  (**5**) in  $\text{CH}_2\text{Cl}_2$  solution ( $[\text{5}]_0 = 0.005 \text{ mol/dm}^3$ ) between 2110 and  $1700 \text{ cm}^{-1}$  under an atmospheric pressure of  $^{13}\text{CO}$  at  $10^\circ\text{C}$  using a  $0.0218 \text{ cm}$   $\text{CaF}_2$  liquid cell: (blue line) reaction time 65 s; (violet line) reaction time 1080 s; (green line) reaction time 2135 s; (black line) reaction time 7585 s.

conditions ( $40^\circ\text{C}$ , in the dark) the above transformations need more than 24 h for completion.

Figure 3 shows that under an atmosphere of  $^{13}\text{CO}$  at  $10^\circ\text{C}$  in the dark the intensity of the  $2010 \text{ cm}^{-1}$  band of complex **5** remained practically unchanged for more than 2 h but the intensity of the band at  $1889 \text{ cm}^{-1}$  decreased dramatically and was shifted to lower wavenumbers. The initial rate of CO exchange based on the decrease of intensity of the band at  $1889$  is  $0.44 \times 10^{-5} \text{ mol of CO}/(\text{dm}^3 \text{ s})$ .

The solvent-free reaction product of the  $^{13}\text{CO}$  exchange experiment stored in the refrigerator for 10 days shows, according to its infrared spectrum, a complete scrambling of  $^{13}\text{CO}$  not only in the anionic part of  $[\text{Co}(\text{CO})_3(\text{PPh}_3)_2][\text{Co}(\text{CO})_4]$  but in the cationic part as well. High  $^{13}\text{CO}$  enrichment (ca. 75%) in both parts of  $[\text{Co}(\text{CO})_3(\text{PPh}_3)_2][\text{Co}(\text{CO})_4]$  was achieved by preparing  $^{13}\text{CO}$ -enriched (ca. 75%)  $\text{Co}_2(\text{CO})_8$  in  $\text{CH}_2\text{Cl}_2$  solution at first and then adding 2 equiv of  $\text{PPh}_3$  to form the disproportionation product. The CO ligands of  $^{13}\text{CO}$ -enriched  $[\text{Co}(\text{CO})_3(\text{PPh}_3)_2][\text{Co}(\text{CO})_4]$  show  $^{13}\text{C}$  resonances at  $214.10$  (octet,  $^1J(^{13}\text{C}-^{59}\text{Co}) = 280.1 \text{ Hz}$ ) and  $193.64 \text{ ppm}$  (triplet,  $^2J(^{31}\text{P}-^{13}\text{C}) = 24.9 \text{ Hz}$ ) and a  $^{31}\text{P}$  resonance at  $54.79 \text{ ppm}$  (quartet,  $^2J(^{31}\text{P}-^{13}\text{C}) = 12.5 \text{ Hz}$ ).

Repeating the carbonylation experiment of ethyl diazoacetate in the absence of ethanol but under a  $^{13}\text{CO}$  atmosphere (Figure 4) confirmed the relatively rapid CO exchange in the anionic part of complex **5** shown in Figure 3 and the correlation shown in Figure 2. In comparison to Figure 2 the results in Figure 4 show that under  $^{13}\text{CO}$  the appearance of the  $1734 \text{ cm}^{-1}$  band of the ketene dimer is unchanged but the band at  $1637 \text{ cm}^{-1}$  is shifted to  $1606 \text{ cm}^{-1}$ .

We found that not only  $[\text{Co}(\text{CO})_3(\text{PPh}_3)_2][\text{Co}(\text{CO})_4]$  but also  $[\text{Co}(\text{EtOH})_6][\text{Co}(\text{CO})_4]_2$  and  $\text{Na}[\text{Co}(\text{CO})_4]$  are active catalyst precursors. Their catalytic activity in the carbonylation of ethyl diazoacetate, however, is lower than that observed with  $[\text{Co}(\text{CO})_3(\text{PPh}_3)_2][\text{Co}(\text{CO})_4]$ . On the other hand, the complex  $[\text{PPN}][\text{Co}(\text{CO})_4]^{22}$  ( $\text{PPN} = [\text{Ph}_3\text{P}=\text{N}=\text{PPh}_3]^+$ ) shows no catalytic activity in the carbonylation reaction at all (Table 2). A comparison of the rates of carbonylation ( $r_{\text{DEM}}$ ) with those of CO exchange ( $r_{\text{CO exchange}}$ ) measured under a  $^{13}\text{CO}$  atmosphere for the four different complexes of

$[\text{Co}(\text{CO})_4]^-$  shows no parallelism between the rates. With respect to the rates of  $^{13}\text{CO}$  exchange,  $\text{Na}[\text{Co}(\text{CO})_4]$  shows the highest activity, in accord with our earlier observation,<sup>40</sup> and complex  $[\text{Co}(\text{CO})_3(\text{PPh}_3)_2][\text{Co}(\text{CO})_4]$  shows the lowest activity. The rates of  $^{13}\text{CO}$  exchange with the complexes  $[\text{Co}(\text{EtOH})_6][\text{Co}(\text{CO})_4]_2$  and  $[\text{PPN}][\text{Co}(\text{CO})_4]$  are between those observed with  $[\text{Co}(\text{CO})_3(\text{PPh}_3)_2][\text{Co}(\text{CO})_4]$  and  $\text{Na}[\text{Co}(\text{CO})_4]$ . In the presence of 100 and 50 mol % cobaltocene the complexes **5** and **7** (entries 1, 2 and entries 3, 5, respectively) show little change in activities in the CO exchange and in the ethyl diazoacetate carbonylation reactions. Complexes **8** and **9**, however, show strongly diminished activities in these reactions if 50 mol % cobaltocene is present (entries 6–8).

Commercially available polystyrenediphenylphosphane (PSDP) ( $1.6 \text{ mmol P/g}$ ;  $100\text{--}200$  mesh particle size) swollen in  $\text{CH}_2\text{Cl}_2$  was treated with solutions of  $\text{Co}_2(\text{CO})_8$  in  $\text{CH}_2\text{Cl}_2$  at room temperature. A mixture of the polymer-bound analogues of the complexes  $[\text{Co}(\text{CO})_3(\text{PPh}_3)_2][\text{Co}(\text{CO})_4]$  (**5**) and  $\text{Co}_2(\text{CO})_7(\text{PPh}_3)$  (**1**) was obtained as red-brown beads after drying. Infrared spectra in Nujol mull and KBr pellet confirmed the presence of the polymer-bound complexes. The ratio of the polymer-bound complexes in the loaded polymer was calculated from the material balance (see the Experimental Section), which was in accord with the result of Co and P analyses. Using this material as the catalyst in the carbonylation of ethyl diazoacetate in  $\text{CH}_2\text{Cl}_2$  solution give the best results at  $40^\circ\text{C}$  under 11 bar of CO pressure (see Table 3 for the results under various reaction conditions). Complete conversion into diethyl malonate was achieved, and no cobalt leaching from the catalyst into the solution of the product was observed by infrared spectroscopy. Turnover frequencies up to  $5.1 \text{ mol}/(\text{mol h})$  were achieved. The catalyst can be recycled, but the activity decreases in the consecutive cycles (see entries 12–16). According to ICP-OES analyses of the catalyst after the fifth cycle the phosphorus content is practically unchanged but the cobalt content drops to 95.8% of the original value. In the absence

(40) Ungváry, F.; Wojcicki, A. *J. Am. Chem. Soc.* **1987**, *109*, 6848–6849.



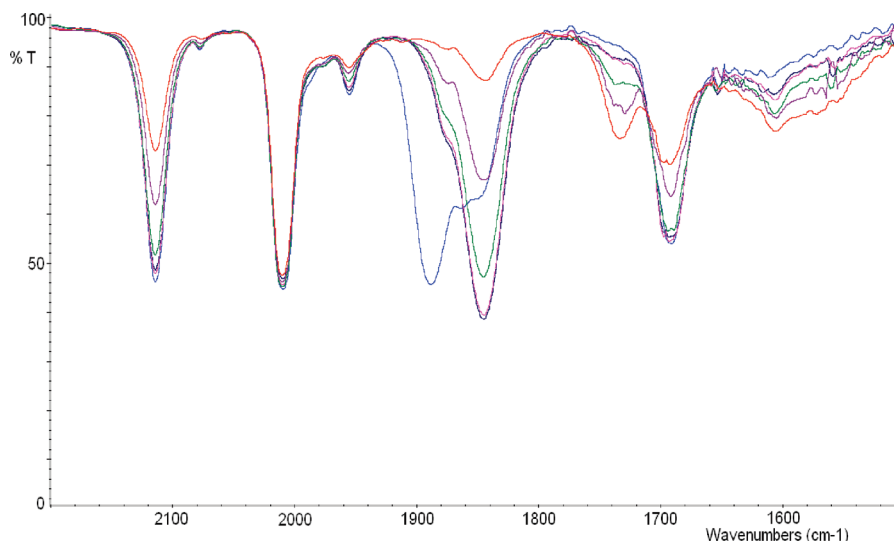


**Figure 4.** Change of the infrared spectra between 2200 and 1500  $\text{cm}^{-1}$  during the catalytic carbonylation of ethyl diazoacetate (EDA) in the absence of ethanol with  $[\text{Co}(\text{CO})_3(\text{PPh}_3)_2][\text{Co}(\text{CO})_4]$  (**5**) as the catalyst precursor under atmospheric pressure of  $^{13}\text{CO}$  at 10 °C in  $\text{CH}_2\text{Cl}_2$  solution using a 0.021 80 cm  $\text{CaF}_2$  liquid cell: (blue line) reaction time 5 min; (light violet line) reaction time 30 min; (dark blue line) reaction time 60 min; (green line) reaction time 120 min; (dark violet line) reaction time 180 min; (red line) reaction time 240 min. Initial concentrations:  $[\text{EDA}]_0 = 0.0186 \text{ mol/dm}^3$ ,  $[\text{5}]_0 = 0.0043 \text{ mol/dm}^3$ ,  $[^{13}\text{CO}]_0 = 0.00508 \text{ mol/dm}^3$ .

**Table 2.** Initial Rate of  $^{13}\text{CO}$  Exchange ( $r_{\text{CO exchange}}^a$ ) and the Initial Rate of Diethyl Malonate Formation ( $r_{\text{DEM}}^b$ ) in the Presence of Different Complexes of Tetracarbonylcobaltate(−):  $[\text{Co}(\text{CO})_3(\text{PPh}_3)_2][\text{Co}(\text{CO})_4]$  (**5**),  $[\text{Co}(\text{EtOH})_6][\text{Co}(\text{CO})_4]_2$  (**7**),  $\text{Na}[\text{Co}(\text{CO})_4]$  (**8**), and  $[\text{PPN}][\text{Co}(\text{CO})_4]$  (**9**) under Atmospheric Pressure (736–745 mmHg) of  $^{13}\text{CO}$  and CO, Respectively, in  $\text{CH}_2\text{Cl}_2$  Solution at 10 °C

complex	entry	$[\text{Co}(\text{CO})_4]_0$ (mol/dm <sup>3</sup> )	$10^2[\text{CO}]_0^c$ (mol/dm <sup>3</sup> )	$10^5 r_{\text{CO exchange}}^a$ (mol/(dm <sup>3</sup> s))	$10^5 r_{\text{DEM}}^b$ (mol/(dm <sup>3</sup> s))
<b>5</b>	1	0.005	0.504		3.47 (3.19) <sup>d</sup>
	2	0.005	0.508 <sup>a</sup>	0.44 (0.47) <sup>d</sup>	
<b>7</b>	3	0.008	0.790 <sup>a</sup>	2.34 <sup>e</sup> (2.23) <sup>f</sup>	
	4	0.005	0.802		0.16 <sup>e</sup>
	5	0.050	0.790		1.70 <sup>e</sup> (1.41) <sup>f</sup>
<b>8</b>	6	0.005	0.760 <sup>a</sup>	3.67 <sup>g</sup> (0.04) <sup>f</sup>	
	7	0.005	0.760		1.68 <sup>g</sup> (0.10) <sup>f</sup>
<b>9</b>	8	0.005	0.510 <sup>a</sup>	1.50 (0.01) <sup>f</sup>	
	9	0.005	0.510		<0.001

<sup>a</sup> The CO exchange reaction started under an atmosphere of  $^{13}\text{CO}$  at 743 mmHg total pressure. <sup>b</sup> Carbonylation reaction of ethyl diazoacetate (EDA) started with  $[\text{EDA}]_0 = [\text{EtOH}]_0 = 0.25 \text{ mol/dm}^3$  under an atmosphere of CO. <sup>c</sup> Calculated from the partial pressure of CO and the known solubility of CO in  $\text{CH}_2\text{Cl}_2$ <sup>41,42</sup> expressed in mole fraction:  $x_{\text{CO}}(10^\circ\text{C}, 1 \text{ bar of } P(\text{CO})) = 0.000473$  converted to  $[\text{CO}] = 0.007489 \text{ mol/dm}^3$ . Solubility of CO in EtOH<sup>43</sup> expressed in mole fraction:  $x_{\text{CO}}(10^\circ\text{C}, 1 \text{ bar of } P(\text{CO})) = 0.000487$  converted to  $[\text{CO}] = 0.008438 \text{ mol/dm}^3$ . The solubility of CO in THF  $[\text{CO}](10^\circ\text{C}, 1 \text{ bar of } P(\text{CO})) = 0.0087 \pm 0.0011$  was extrapolated from published values at 30 and 25 °C.<sup>44</sup> <sup>d</sup> In the presence of 100 mol % cobaltocene. <sup>e</sup> Reactions performed in EtOH solutions. <sup>f</sup> In the presence of 50 mol % cobaltocene. <sup>g</sup> Reactions performed in THF solutions.

of ethanol nearly complete conversion into 3-(ethoxycarbonyl)-4-hydroxy-6-ethoxy-2H-pyran-2-one (dimer of (ethoxycarbonyl)ketene) was obtained (entry 11).

Using  $\text{CH}_2\text{Cl}_2$  solutions of the complex  $\text{Co}_2(\text{CO})_7(\text{CHCO}_2\text{Et})$  for the cobalt loading onto PSDP, we obtained the polymer-bound analogue of the complex  $\text{Co}_2(\text{CO})_6(\text{CHCO}_2\text{Et})(\text{PPh}_3)$  (**3**) as dark red beads. This catalyst shows activity in the carbonylation of ethyl diazoacetate lower than that observed by using the mixture of 88% PSDP-anchored “ $[\text{Co}(\text{CO})_3(\text{PPh}_3)_2][\text{Co}(\text{CO})_4]$ ” and 12% PSDP-anchored “ $\text{Co}_2(\text{CO})_7(\text{PPh}_3)$ ” under the same reaction conditions (cf. the results in Table 4 with those in Table 3). However, despite its lower activity, the polymer-bound analogue of the complex  $\text{Co}_2(\text{CO})_6(\text{CHCO}_2\text{Et})(\text{PPh}_3)$  is also a suitable catalyst for the carbonylation of ethyl diazoacetate.

In order to have a comparison of the activity of the polymer-bound catalysts with those of the corresponding

isolated complexes, we performed experiments with the latter at 40 °C as well. The data in Table 5 show that the complexes **3**, **1**, and **5** in 0.005 mol/dm<sup>3</sup> concentration are up to 2 orders of magnitude more active under these conditions than the polymer-bound complexes applied in 0.05 mmol quantities/cm<sup>3</sup> in the reaction mixture. Using complex **6** as the catalyst precursor under the same conditions, a lower yield and turnover frequency was observed than with the other complexes (cf. entry 3 with entries 1, 2, and 4). At the end of 1 h reaction time the infrared spectrum of the reaction mixture shows the almost complete conversion of complex **6** into complex **1**.

The  $^{31}\text{P}$  resonances of dichloromethane-swelled polystyrenediphenylphosphane (PSDP) beads are at −7.2 (60%) and

(42) Magee, M. P.; Li, H.-Q.; Morgan, O.; Hersh, W. H. *Dalton Trans.* **2003**, 387–394.

(43) Cargill, R. W., Ed. *IUPAC Solubility Data Series*; Pergamon Press: Oxford, U.K., 1990; Vol. 43 (Carbon Monoxide), p 166.

(44) Payne, M. W.; Leussing, D. L.; Shore, S. G. *J. Am. Chem. Soc.* **1987**, 109, 617–618.

(41) Jonasson, A.; Persson, O.; Rasmussen, P. *J. Chem. Eng. Data* **2000**, 45, 642–646.



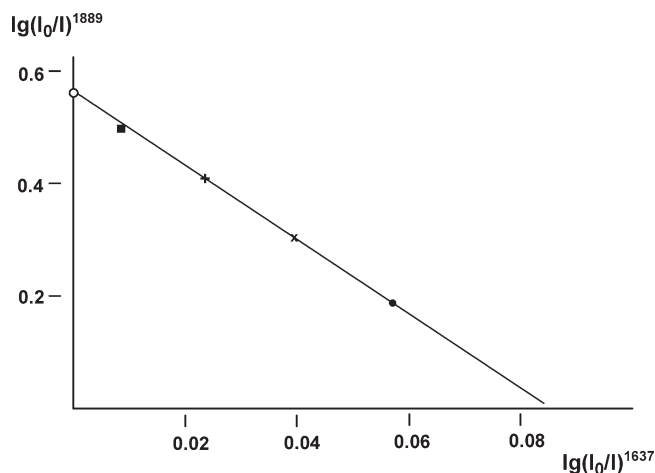


**Figure 5.** Correlation of the infrared band intensities at 1889 and 1637  $\text{cm}^{-1}$  in  $[\text{Co}(\text{CO})_3(\text{L})]^-$  ( $\text{L} = \text{CHCO}_2\text{Et}$ ,  $\text{O}=\text{C}=\text{CHCO}_2\text{Et}$ ) of a reaction mixture with the initial concentrations  $[\mathbf{5}]_0 = 0.0045 \text{ mol/dm}^3$ ,  $[\text{N}_2\text{CHCO}_2\text{Et}]_0 = 0.0182 \text{ mol/dm}^3$ , and  $[\text{CO}]_0 = 0.00504 \text{ mol/dm}^3$  as measured at the beginning (○) and at 66 (■), 134 (+), 193 (×) and 265 min (●) reaction time using a 0.0218 cm  $\text{CaF}_2$  liquid cell. **5** denotes the complex  $[\text{Co}(\text{CO})_3(\text{PPh}_3)_2]^-[\text{Co}(\text{CO})_4]$ .

−8.0 (40%) (lit.<sup>45</sup> −5.4 ppm for  $\text{PPh}_3$ ). The dichloromethane-swelled beads of the PSDP-bound phosphazane show a  $^{31}\text{P}$  resonance at 19.3 ppm (lit.<sup>46</sup> 22.7 ppm for  $\text{Ph}_3\text{P}=\text{NN}=\text{CHCO}_2\text{Et}$ ). These signals are completely absent in the PSDP-bound cobalt catalysts being used in carbonylation experiments of ethyl diazoacetate.

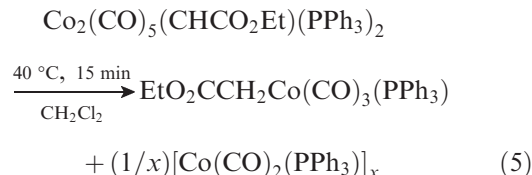
#### 4. Discussion

The carbonylation of ethyl diazoacetate using complex **1** or complex **3** as the catalyst precursor can be explained on the basis of the observed negative effect of CO and on the basis of the observed cobalt complexes in the reaction mixture during catalysis by a catalytic cycle in which  $\text{Co}_2(\text{CO})_6(\text{PPh}_3)$  and  $\text{Co}_2(\text{CO})_6(\text{CHCO}_2\text{Et})(\text{PPh}_3)$  are the repeating species (Scheme 2).

The suggested catalytic cycle shown in Scheme 2 can be put into effect in two ways: either by adding complex **1** or by adding complex **3** to the reaction mixture. The presence of both complexes can be seen by infrared spectroscopy during the catalytic reaction. We have already shown that the (ethoxycarbonyl)carbene ligand in complex **3** can be driven out by CO with the simultaneous quantitative formation of complex **1** and diethyl malonate (if equimolar amounts of ethanol were also present).<sup>12</sup> The bottleneck of the cycle is most probably the dediazotization of ethyl diazoacetate by complex **1**. The observed negative effect of carbon monoxide on the rate of the reaction suggests that the actual reaction partner of ethyl diazoacetate in the deazotization reaction is the coordinative unsaturated  $\text{Co}_2(\text{CO})_6(\text{PPh}_3)$  formed in undetectable low concentrations by reversible CO loss from complex **1**. Diethyl malonate is the product of the fast reaction of the (ethoxycarbonyl)ketene intermediate with ethanol. In the absence of ethanol the (ethoxycarbonyl)ketene dimerizes to 3-(ethoxycarbonyl)-4-hydroxy-6-ethoxy-2H-pyran-2-one.<sup>38</sup>

The low activity of complex **6** as the catalyst precursor and its slow conversion during the catalytic reaction into complex **1** does not conform to a catalytic cycle in which complex **6** and  $\text{Co}_2(\text{CO})_5(\text{CHCO}_2\text{Et})(\text{PPh}_3)$  are the repeating species (Scheme 3). Rather, the observed catalytic activity in this case can be assigned to complex **1**, formed from complex **6**.

The facile decomposition of complex **4** in dichloromethane solution at 40 °C gives two distinct products according to eq 5. We assume that the source of the second hydrogen atom in the (ethoxycarbonyl)methyl group of  $\text{EtO}_2\text{CCH}_2\text{Co}(\text{CO})_3(\text{PPh}_3)$  is the solvent. The insoluble byproduct  $[\text{Co}(\text{CO})_2(\text{PPh}_3)]_x$  may be the same as  $[\text{Co}(\text{CO})_2(\text{PPh}_3)]_n$  obtained from  $[\text{Co}(\text{CO})_3(\text{PPh}_3)_2][\text{Co}(\text{CO})_4]$  in refluxing acetone solutions.<sup>47</sup>



Research on various carbonylcobalt cation–anion pairs has revealed already a rich thermal chemistry and photochemistry.<sup>48,49</sup> We believe that the observed high activity of  $[\text{Co}(\text{CO})_3(\text{PPh}_3)_2][\text{Co}(\text{CO})_4]$  (**5**) in catalyzing the carbonylation of ethyl diazoacetate opens an interesting new chapter in the chemistry of this classical homonuclear ion pair.

The lower intensity of the 1889  $\text{cm}^{-1}$  band of complex **5** during the catalytic carbonylation of ethyl diazoacetate suggests that the tetracarbonylcobaltate(−) part of the complex is involved in the deazotization and carbonylation of ethyl diazoacetate. For the deazotization of diazoalkanes metal complexes with a vacant coordination site were found to be active.<sup>50</sup> A vacant coordination site in  $[\text{Co}(\text{CO})_3(\text{PPh}_3)_2][\text{Co}(\text{CO})_4]$  may be formed in the tetracarbonylcobaltate(−) part of the complex, which then transfers the diazoalkane into a carbene ligand and dinitrogen. The reaction of the carbene ligand with carbon monoxide can result in the formation of a ketene ligand. The observed correlation of the decreasing band intensity at 1889  $\text{cm}^{-1}$  with the increasing band intensity of a new absorption at 1637  $\text{cm}^{-1}$  (see Figure 5) might be an indication of intermediate carbene and/or ketene complexes. The good correlation shown in Figure 5 and the absence of new  $\nu(\text{C}=\text{O})$  bands in the vicinity of 1889  $\text{cm}^{-1}$  supports the idea that the  $\nu(\text{C}=\text{O})$  band position of the carbonyl ligands of  $[\text{Co}(\text{CO})_3(\text{L})]^-$  are coincidentally the same as those of  $[\text{Co}(\text{CO})_4]^-$ . The computed average C–O bond distances in  $[\text{Co}(\text{CO})_3(\text{L})]^-$  (1.1640 and 1.1643 Å) are indeed very close to the C–O bond distances in  $[\text{Co}(\text{CO})_4]^-$  (1.1690 Å). The band at 1637  $\text{cm}^{-1}$  can be assigned either to the  $\nu(\text{C}=\text{O})$  of the (ethoxycarbonyl)carbene ligand in  $[\text{Co}(\text{CO})_3(\text{CHCO}_2\text{Et})]^-$  or to the ester  $\nu(\text{C}=\text{O})$  and the ketene  $\nu(\text{C}=\text{O})$  of the (ethoxycarbonyl)ketene

(47) Sacco, A. *Gazz. Chim. Ital.* **1963**, 93, 542–548.

(48) (a) Atwood, J. D. *Inorg. Chem.* **1987**, 26, 2918–2920. (b) Zhen, Y. Q.; Feighery, W. G.; Atwood, J. D. *J. Am. Chem. Soc.* **1991**, 113, 3616–3618.

(49) (a) Bockman, T. M.; Kochi, J. K. *J. Am. Chem. Soc.* **1989**, 111, 4669–4683. (b) Kochi, J. K.; Bockman, T. M. *Adv. Organomet. Chem.* **1991**, 33, 51–124. (c) Wei, C. H.; Bockman, T. M.; Kochi, J. K. *J. Organomet. Chem.* **1992**, 428, 85–97. (d) Kochi, J. K. *Adv. Phys. Org. Chem.* **1994**, 29, 185–272 and references therein.

(50) Doyle, M. P.; McKervy, M. A.; Ye, T. *Modern Catalytic Methods for Organic Synthesis with Diazo Compounds*; Wiley: New York, 1998; pp 62–66.

(45) Albright, T. A.; Freeman, W. J.; Schweizer, E. *J. Org. Chem.* **1976**, 41, 2716–2720.

(46) Pedro, F. M.; Santos, A. M.; Baratta, W.; Kühn, F. E. *Organometallics* **2007**, 26, 302–309.

**Table 3. Yield of Diethyl Malonate (DEM) from Ethyl Diazoacetate (EDA) under Carbon Monoxide Pressure in the Presence of 75 mg (0.05 mmol “Co<sub>2</sub>”) Polystyrenediphenylphosphane (PSDP)-Anchored Carbonyl Cobalt Catalyst (7.87 m/m % Co and 3.68 m/m % P, Corresponding to a Mixture of 88% PSDP-Anchored “[Co(CO)<sub>3</sub>(PPh<sub>3</sub>)<sub>2</sub>][Co(CO)<sub>4</sub>]” and 12% PSDP-Anchored “Co<sub>2</sub>(CO)<sub>7</sub>(PPh<sub>3</sub>)” in 1.0 cm<sup>3</sup> Methylene Chloride Solution under Various Reaction Conditions**

entry	<i>T</i> (°C)	<i>P</i> <sub>total</sub> (bar)	[EDA] <sub>0</sub> (mol/dm <sup>3</sup> )	[EtOH] <sub>0</sub> (mol/dm <sup>3</sup> )	reacn time (h)	yield of DEM <sup>a</sup> (%)	TOF <sup>b</sup> (h <sup>-1</sup> )
1	10	11	0.25	0.30	4	14	0.18
2	25	11	0.25	0.30	4	66	0.83
3	40	11	0.25	0.30	4	100	1.25
4	40	11	0.50	0.60	4	99	2.48
5	40	11	1.00	1.00	4	99	4.95
6	40	11	2.00	2.00	4	50	5.01
7	40	11	4.00	4.00	4	26	5.10
8	40	11	6.00	6.00	4	17	5.10
9	40	5	0.25	0.30	4	95	1.19
10	40	50	0.25	0.30	4	94	1.18
11	40	50	0.25	0.30	4	96 <sup>c</sup>	1.20 <sup>c</sup>
12	40	11	0.25	0.30	4	98	1.23
13	40	11	0.25	0.30	4	97 <sup>d</sup>	1.21
14	40	11	0.25	0.30	16	99 <sup>e</sup>	0.31
15	40	11	0.25	0.30	26	83 <sup>f</sup>	0.16
16	40	11	0.25	0.30	29	61 <sup>g</sup>	0.11

<sup>a</sup> Determined by quantitative infrared spectroscopy using the molar absorbances of DEM in CH<sub>2</sub>Cl<sub>2</sub> at 1730 and 1749 cm<sup>-1</sup> ( $\epsilon_M^{1730\text{ cm}^{-1}} = 666\text{ cm}^2/\text{mmol}$ ,  $\epsilon_M^{1749\text{ cm}^{-1}} = 579\text{ cm}^2/\text{mmol}$ ). <sup>b</sup> In units of mol of product/(mol of catalyst) h). <sup>c</sup> 3-(Ethoxycarbonyl)-4-hydroxy-6-ethoxy-2H-pyran-2-one (dimer of ethoxycarbonylketene), determined by quantitative infrared spectroscopy using the molar absorbance in CH<sub>2</sub>Cl<sub>2</sub> at 1734 cm<sup>-1</sup> ( $\epsilon_M^{1734\text{ cm}^{-1}} = 422\text{ cm}^2/\text{mmol}$ ). The TOF was calculated for the monomer. <sup>d</sup> Catalyst of entry 12 recycled. <sup>e</sup> Catalyst of entry 13 recycled. <sup>f</sup> Catalyst of entry 14 recycled. <sup>g</sup> Catalyst of entry 15 recycled. IPC-OES analysis of the recovered catalyst: 3.65 m/m % P and 7.54 m/m % Co.

**Table 4. Yield of Diethyl Malonate (DEM) from Ethyl Diazoacetate (EDA) under Carbon Monoxide Pressure in the Presence of 51.3 mg (0.05 mmol “Co<sub>2</sub>”) of Polystyrenediphenylphosphane (PSDP)-Anchored “Co<sub>2</sub>(CO)<sub>6</sub>(CHCO<sub>2</sub>Et)(PPh<sub>3</sub>)” (11.10 m/m % Co and 3.02 m/m % P), in 1.0 cm<sup>3</sup> Dichloromethane Solution under Various Reaction Conditions**

entry	<i>T</i> (°C)	<i>P</i> <sub>total</sub> (bar)	[EDA] <sub>0</sub> (mol/dm <sup>3</sup> )	[EtOH] <sub>0</sub> (mol/dm <sup>3</sup> )	reacn time (h)	yield of DEM <sup>a</sup> (%)	TOF <sup>b</sup> (h <sup>-1</sup> )
1	25	11	0.25	0.30	24	14	0.03
2	40	11	0.25	0.30	4	23	0.29
3	40	11	0.25	0.30	24	92	0.20
4	40	11	1.00	1.20	24	95	0.79
5	40	11	2.00	2.00	24	53	0.88
6	40	11	4.00	4.00	24	29	0.97

<sup>a</sup> Determined by quantitative infrared spectroscopy using the molar absorbances of DEM in CH<sub>2</sub>Cl<sub>2</sub> at 1730 and 1749 cm<sup>-1</sup> ( $\epsilon_M^{1730\text{ cm}^{-1}} = 666\text{ cm}^2/\text{mmol}$ ,  $\epsilon_M^{1749\text{ cm}^{-1}} = 579\text{ cm}^2/\text{mmol}$ ). <sup>b</sup> In units of mol of product/(mol of catalyst) h).

**Table 5. Yield of Diethyl Malonate from Ethyl Diazoacetate (EDA) at 1 h Reaction Time in the Presence of Ethanol under 11 bar Total Pressure of Carbon Monoxide at 40 °C in the Presence of Co<sub>2</sub>(CO)<sub>6</sub>(CHCO<sub>2</sub>Et)(PPh<sub>3</sub>) (3), Co<sub>2</sub>(CO)<sub>7</sub>(PPh<sub>3</sub>) (1), Co<sub>2</sub>(CO)<sub>5</sub>(CHCO<sub>2</sub>Et)<sub>2</sub>(PPh<sub>3</sub>) (6), or [Co(CO)<sub>3</sub>(PPh<sub>3</sub>)<sub>2</sub>][Co(CO)<sub>4</sub>] (5) as the Catalyst Precursors in 0.005 mol/dm<sup>3</sup> Initial Concentration and the Calculated Turnover Frequency (TOF)**

entry	catalyst	[EDA] <sub>0</sub> (mol/dm <sup>3</sup> )	[EtOH] <sub>0</sub> (mol/dm <sup>3</sup> )	[EDA] <sub>0</sub> /[catalyst] <sub>0</sub>	yield of DEM <sup>a</sup> (%)	TOF <sup>b</sup> (h <sup>-1</sup> )
1	<b>3</b>	0.25	0.30	50	76	60
2	<b>1</b>	0.25	0.30	50	70	35
3	<b>6</b>	0.25	0.30	50	10	4
4	<b>5</b>	0.25	0.30	50	29	15
5	<b>5</b>	0.50	0.60	100	19	19
6	<b>5</b>	1.00	1.20	200	19	38
7	<b>5</b>	2.50	3.00	500	19	95
8	<b>5</b>	5.00	5.00	1000	10	101

<sup>a</sup> Determined by quantitative infrared spectroscopy using the molar absorbances of DEM in CH<sub>2</sub>Cl<sub>2</sub> at 1730 and 1749 cm<sup>-1</sup> ( $\epsilon_M^{1730\text{ cm}^{-1}} = 666\text{ cm}^2/\text{mmol}$ ,  $\epsilon_M^{1749\text{ cm}^{-1}} = 579\text{ cm}^2/\text{mmol}$ ) after 1 h reaction time. <sup>b</sup> In units of mol of product/(mol of catalyst) h).

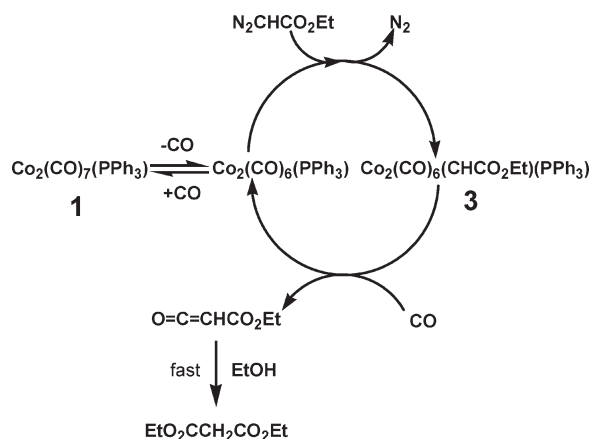
ligand in [Co(CO)<sub>3</sub>(O=C=CHCO<sub>2</sub>Et)]<sup>-</sup>. The shift of the observed band at 1637 cm<sup>-1</sup> to 1606 cm<sup>-1</sup> in the experiment performed under <sup>13</sup>CO supports the assumption that we see in the IR spectra an anionic ketene complex rather than an anionic carbene complex. The existence of [Co(CO)<sub>3</sub>(CHCO<sub>2</sub>Et)]<sup>-</sup> and [Co(CO)<sub>3</sub>(O=C=CHCO<sub>2</sub>Et)]<sup>-</sup> has not been described in the literature so far. The only

anionic cobalt carbonyl carbene complexes known at present are those having an alkyl or an aryl isocyanide ligand.<sup>51</sup> These complexes were prepared by the reaction of alkyl and aryl isocyanides with the highly reduced tricarbonylcobaltate(3-) anion. Examples of anionic ketene complexes of some transition metals are also known.<sup>52</sup>

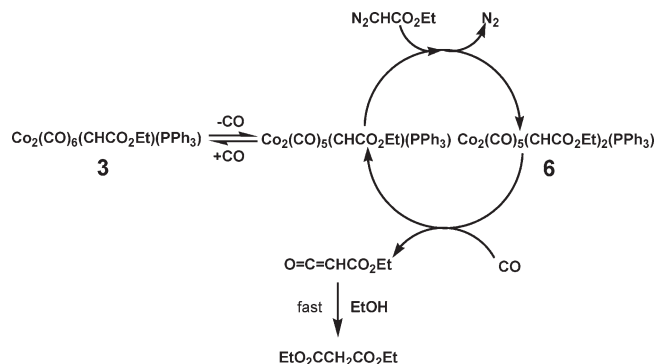
(51) Ellis, J. E.; Barger, P. T.; Winzenburg, M. L.; Warnock, G. F. *J. Organomet. Chem.* **1990**, 383, 521–530.

(52) Geoffroy, G. L.; Bassner, S. L. *Adv. Organomet. Chem.* **1988**, 28, 1–83.

**Scheme 2. Suggested Mechanism for Catalytic Diethyl Malonate Formation using  $\text{Co}_2(\text{CO})_7(\text{PPh}_3)$  or  $\text{Co}_2(\text{CO})_6(\text{CHCO}_2\text{Et})(\text{PPh}_3)$  as the Precatalyst for the Carbonylation of Ethyl Diazoacetate**



**Scheme 3. Tentative Mechanism for the Carbonylation of Ethyl Diazoacetate using  $\text{Co}_2(\text{CO})_6(\text{CHCO}_2\text{Et})(\text{PPh}_3)$  or  $\text{Co}_2(\text{CO})_5(\text{CHCO}_2\text{Et})_2(\text{PPh}_3)$  as the Catalyst Precursor**



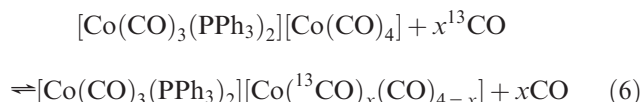
According to the correlation shown in Figure 5 a log  $I_0/I$  value of 0.0214 at  $1637\text{ cm}^{-1}$  corresponds to a composition of  $[\text{Co}(\text{CO})_3(\text{PPh}_3)_2][\text{Co}(\text{CO})_3(\text{L})]$  with  $0.0045\text{ mol/dm}^3$  concentration. Taking into account the thickness of the applied solution cell ( $0.0218\text{ cm}$ ), a molar absorbance of  $\epsilon_{\text{M}}^{1637\text{ cm}^{-1}} = 218\text{ cm}^2/\text{mmol}$  can be calculated for the supposed  $[\text{Co}(\text{CO})_3(\text{PPh}_3)_2][\text{Co}(\text{CO})_3(\text{L})]$  at  $1637\text{ cm}^{-1}$ .

Since the concentrations of CO and  $\text{PPh}_3$  have a negative effect on the rate of the catalytic carbonylation of ethyl diazoacetate, we assume the reversible formation of the  $[\text{Co}(\text{CO})_3(\text{PPh}_3)_2][\text{Co}(\text{CO})_3]$  intermediate. Reaction of this intermediate with ethyl diazoacetate might initiate the deazotization of ethyl diazoacetate and the formation of the corresponding complex carbenoid  $[\text{Co}(\text{CO})_3(\text{PPh}_3)_2][\text{Co}(\text{CO})_3(\text{CHCO}_2\text{Et})]$ , which upon reaction with CO (external or coordinated) gives (ethoxycarbonyl)ketene, and a new cycle can start according to Scheme 4.

The observed zero-order ethanol dependence of the diethyl malonate formation suggests that the reaction of (ethoxycarbonyl)ketene with ethanol is faster than its formation in the catalytic cycle. In the absence of ethanol (ethoxycarbonyl)ketene dimerizes into 3-(ethoxycarbonyl)-4-hydroxy-6-ethoxy-2H-pyran-2-one.<sup>38</sup>

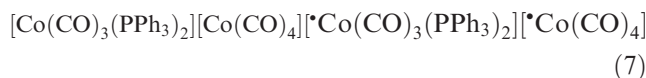
Although the CO exchange in the anionic part of complex 5 observed in the presence of  $^{13}\text{CO}$  according to eq 6 occurs on a time scale similar to that for the catalytic carbonylation

of ethyl diazoacetate, different mechanisms might operate in each case.



It is known that the carbonyl ligands in  $\text{Na}[\text{Co}(\text{CO})_4]$  can be substituted by  $^{13}\text{CO}$ , phosphites, phosphanes, and activated olefins in facile thermal and photochemical reactions.<sup>40,53</sup> According to theoretical calculations the thermal formation of  $[\text{Co}(\text{CO})_3]^-$  from  $[\text{Co}(\text{CO})_4]^-$  by CO dissociation needs too much energy ( $42.4\text{ kcal/mol}^{54}$ ). The observation that the presence of catalytic amounts of  $\text{Co}_2(\text{CO})_8$  or  $\text{Co}_4(\text{CO})_{12}$  are necessary for the  $^{13}\text{CO}$  scrambling in  $[\text{Co}(\text{CO})_4]^-$ <sup>55</sup> suggests an energetically much favorable radical pathway with the involvement of the tetracarbonylcobalt radical in both  $^{13}\text{CO}$  scrambling and in the reaction with ethyl diazoacetate. For the former the reactions in Scheme 5 and for the latter the reaction sequence in Scheme 6 seem to be more favorable. Essential for keeping the reaction catalytic in both cases are the facile one-electron exchange reactions between the 17e radical species and the tetracarbonylcobaltate(−) ion in the final steps. Traces of oxygen can serve for the initial formation of the tetracarbonylcobalt radical by oxidation of  $\text{Na}[\text{Co}(\text{CO})_4]$  and of  $[\text{PPN}][\text{Co}(\text{CO})_4]$ . In accord with this idea is the experimental observation that there are strongly diminished rates of  $^{13}\text{CO}$  scrambling and ethyl diazoacetate carbonylation if the highly reducing cobaltocene is present in the reaction mixture in the case of  $\text{Na}[\text{Co}(\text{CO})_4]$  and of  $[\text{PPN}][\text{Co}(\text{CO})_4]$ .

For the formation of  $[\text{Co}(\text{CO})_4]^\bullet$  the presence of  $\text{Co}_2(\text{CO})_8$  is not necessary in the case of complex 5. The transfer of an electron from  $[\text{Co}(\text{CO})_4]^-$  to  $[\text{Co}(\text{CO})_3(\text{PPh}_3)_2]^+$  in complex 5 under thermal or photochemical conditions results in the formation of a radical pair according to eq 7. Hence, radical pathways such as those in Schemes 5 and 6 may work by starting with complex 5 alone in the absence of  $\text{Co}_2(\text{CO})_8$ .



A similar one-electron transfer may occur from  $[\text{Co}(\text{CO})_4]^-$  to  $[\text{Co}(\text{EtOH})_6]^{2+}$  in complex 7 as well. Interestingly, in contrast to the observations with the complexes  $\text{Na}[\text{Co}(\text{CO})_4]$  and  $[\text{PPN}][\text{Co}(\text{CO})_4]$  the presence of cobaltocene does not affect the catalytic activities of complexes 5 and 7 in the CO exchange and in the ethyl diazoacetate carbonylation reaction significantly.

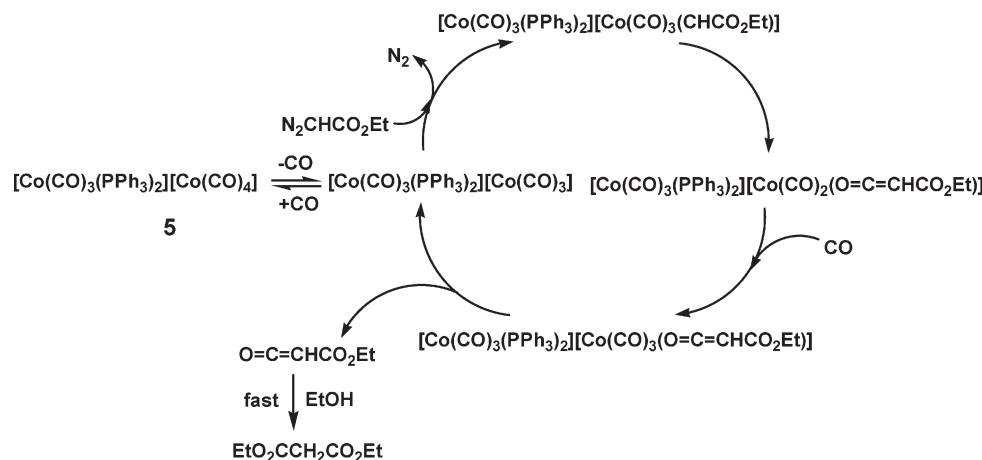
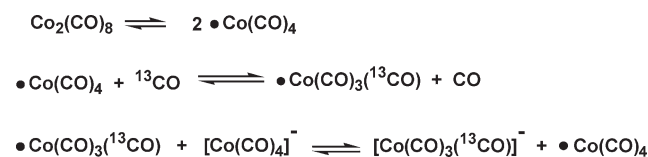
**4.1. Computational Results of the CO Exchange Reaction of  $[\text{Co}(\text{CO})_4]^-$  and  $[\text{Co}(\text{CO})_4]^\bullet$ .** In order to check the likelihood of the involvement of anionic and/or radical carbonyl cobalt species in the  $^{13}\text{CO}$  scrambling and in the carbonylation reactions, we performed theoretical calculations. The most appealing difference in the structures of the anionic  $[\text{Co}(\text{CO})_4]^-$  (10) and the radical  $[\text{Co}(\text{CO})_4]^\bullet$  (10r) is the significant difference in cobalt–carbon bond lengths (see Figure 6), as it

(53) Ungváry, F.; Gallucci, J.; Wojcicki, A. *Organometallics* **1991**, *10*, 3053–3062.

(54) Huo, C. F.; Li, Y. W.; Wu, G. S.; Beller, M.; Jiao, H. *J. Phys. Chem. A* **2002**, *106*, 12161–12169.

(55) Fachinetti, G.; Funaioli, T. *Angew. Chem., Int. Ed. Engl.* **1992**, *31*, 1596–1599.



**Scheme 4. Suggested Mechanism for the Catalytic Diethyl Malonate Formation using  $[\text{Co}(\text{CO})_3(\text{PPh}_3)_2][\text{Co}(\text{CO})_4]$  (**5**) as the Precatalyst for the Carbonylation of Ethyl Diazoacetate****Scheme 5. Suggested Radical Pathway for the  $^{13}\text{CO}$  Exchange in  $[\text{Co}(\text{CO})_4]^-$** 

is remarkably short (1.769 Å) in **10**, whereas the distance of the longer Co–C bond in **10r** is 1.858 Å. The anionic complex  $[\text{Co}(\text{CO})_4]^-$  possesses  $T_d$  symmetry, whereas  $\bullet\text{Co}(\text{CO})_4$  has a trigonal-pyramidal  $C_{3v}$  structure, in accord with earlier theoretical results.<sup>54</sup> The much higher bond dissociation free energy ( $\Delta G_d$ ) for **10** than for **10r** is in line with the difference in Co–C bond lengths in the two complexes. For  $[\text{Co}(\text{CO})_4]^-$   $\Delta G_d = 35.0$  kcal/mol in the gas phase and  $\Delta G_d = 32.0$  kcal/mol when solvation effects are estimated, considering dichloromethane as solvent. For the 17e complex  $\bullet\text{Co}(\text{CO})_4$  the corresponding gas-phase and solvated dissociation free energies are 15.2 and 14.5 kcal/mol, respectively. These results support the idea that the 15e  $\bullet\text{Co}(\text{CO})_3$  complex (**11r**) is involved in both CO exchange and diazo activation.

However, for CO exchange of **10r** an alternative reaction route seems more favorable than the dissociative pathway. CO addition and the dissociation of a carbonyl ligand can take place following an  $\text{S}_{\text{N}}2$ -like reaction mechanism via transition structure **12rTS** with  $D_{3h}$  symmetry. The free energy barrier for this process is 7.4 kcal/mol. Including solvation effects, the activation free energy is slightly elevated to 7.7 kcal/mol. The somewhat similar  $\text{S}_{\text{N}}2$ -like transition structure **12TS** was found for the CO exchange of **10** as well; however, the free energy is much higher than that for the radical pathway, namely 40.8 kcal/mol, and 43.6 kcal/mol when solvation correction is applied. Instead of a  $D_{3h}$  transition state, **12TS** possesses  $C_2$  symmetry with the shortest Co–C bond as the rotation axis.

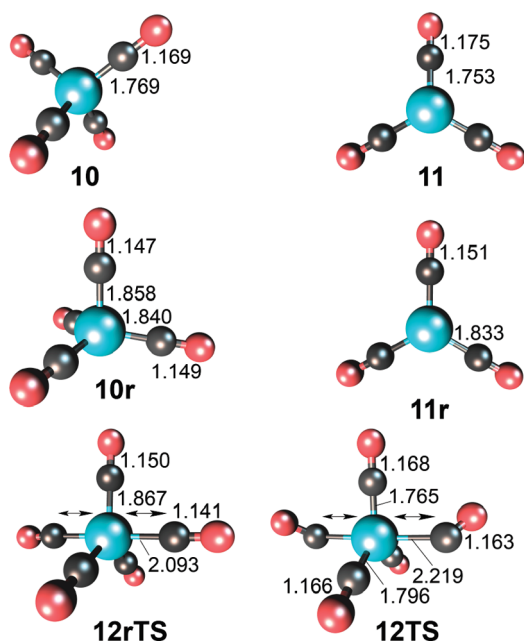
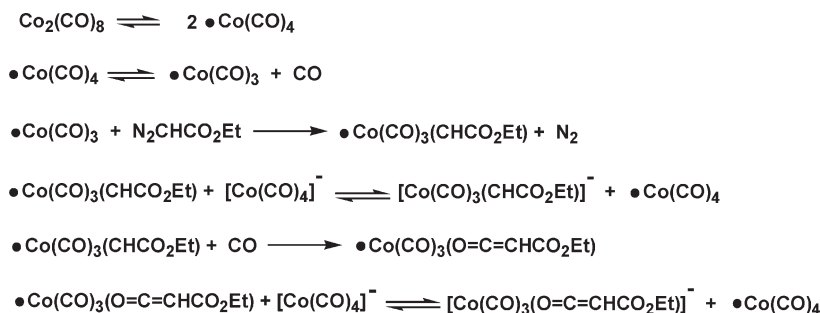
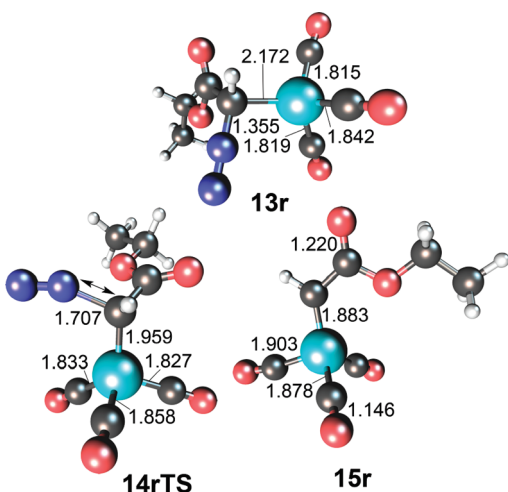
**4.2. Computational Results of the Diazo Activation and Ketene formation.** We made several attempts to find a diazo activation pathway with an  $\text{S}_{\text{N}}2$ -like reaction mechanism starting from **10r** and ethyl diazoacetate (EDA), but no transition state similar to **12rTS** was found, suggesting the dissociative mechanism to be the only viable pathway. Thus, for the diazo activation step the transition state **14rTS** was

found on the  $\bullet\text{Co}(\text{CO})_3(\text{N}_2\text{CHCOOEt})$  potential energy hypersurface, which describes the coordination of EDA on the  $\alpha$ -carbon to the cobalt center with simultaneous  $\text{N}_2$  extrusion. The characteristic single imaginary frequency for **14rTS** is  $533i$   $\text{cm}^{-1}$ . IRC calculations revealed that **14rTS** is connected with **13r**, a diazo complex with an  $\eta^1$  coordination mode. The formation of **13r** from **11r** and EDA is endothermic in terms of free energy by 6.7 kcal/mol (6.4 kcal/mol in gas phase). The free energy barrier for the  $\text{N}_2$  extrusion and carbene formation was found to be 15.6 kcal/mol for the gas phase and 16.4 kcal/mol including solvation effects. The reaction of **11r** with EDA results in carbene complex **15r** possessing  $C_s$  symmetry with a reaction free energy of  $-20.0$  kcal/mol ( $-21.7$  kcal/mol in gas phase). The structures of **13r**, **14rTS**, and **15r** are depicted in Figure 7.

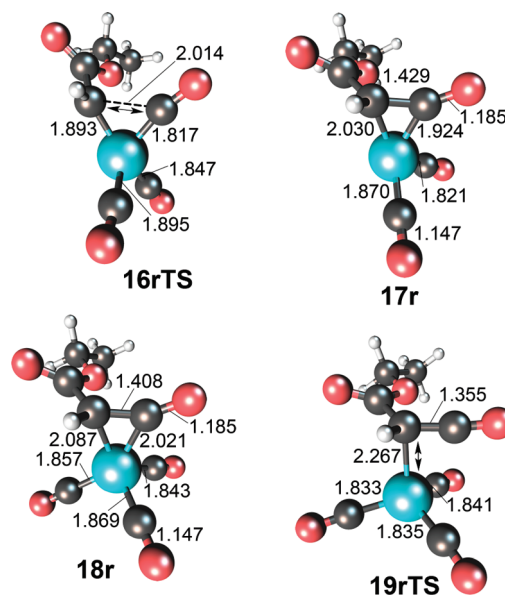
The carbene group in **15r** couples with one of the CO ligands connected to the cobalt center with shorter bond length (1.878 Å). The intramolecular reaction takes place via transition state **16rTS** with a free energy barrier of 15.5 kcal/mol (16.9 kcal/mol in the gas phase). The characteristic imaginary frequency for **16rTS** is  $424i$   $\text{cm}^{-1}$ . The CO–carbene coupling results in the 15e species **17r** with a reaction free energy of  $-7.0$  kcal/mol ( $-5.1$  kcal/mol in the gas phase). Complex **17r** takes up one CO in an exothermic reaction (the reaction free energy is predicted to be  $-12.9$  kcal/mol in the dichloromethane phase and  $-14.5$  kcal/mol in the gas phase), resulting in the 17e complex **18r**. The ketene elimination step is predicted to be exothermic as well, with a free energy of  $-3.2$  kcal/mol ( $-2.0$  kcal/mol in the gas phase). This step proceeds in a fast reaction, as the free energy barrier is only 5.1 kcal/mol (5.2 kcal/mol in the gas phase). The characteristic imaginary frequency for the transition structure **19rTS** describing the ketene dissociation is  $338i$   $\text{cm}^{-1}$ . Intrinsic reaction coordinate (IRC) calculations revealed that **19rTS** indeed connects **18r** with the dissociated (ethoxycarbonyl)ketene along with the coordinatively unsaturated **11r**, which is ready to take up EDA, thus closing the catalytic cycle. The minima and the transition-state structures involved in the ketene formation and elimination step are depicted in Figure 8.

The calculated free energy profile of the ketene formation reaction catalyzed by  $\bullet\text{Co}(\text{CO})_3$  is shown in Figure 9.

The entire anionic pathway has been computed as well in order to make a comparison with the radical ketene

Scheme 6. Suggested Radical Pathway for the Formation of  $[\text{Co}(\text{CO})_3(\text{CHCO}_2\text{Et})]^-$  and  $[\text{Co}(\text{CO})_3(\text{O}=\text{C}=\text{CHCO}_2\text{Et})]^-$ Figure 6. Computed structures of  $[\text{Co}(\text{CO})_4]^-$  (**10**),  $[\text{Co}(\text{CO})_3]^-$  (**11**),  $\bullet\text{Co}(\text{CO})_4$  (**10r**),  $\bullet\text{Co}(\text{CO})_3$  (**11r**), and the transition states **12rTS** and **12TS**. Bond distances are given in Å.Figure 7. Computed structure of the diazo adduct **13r**, transition state **14rTS**, and carbene complex  $\bullet\text{Co}(\text{CO})_3(\text{CHCOOEt})$  (**15r**). Bond distances are given in Å.

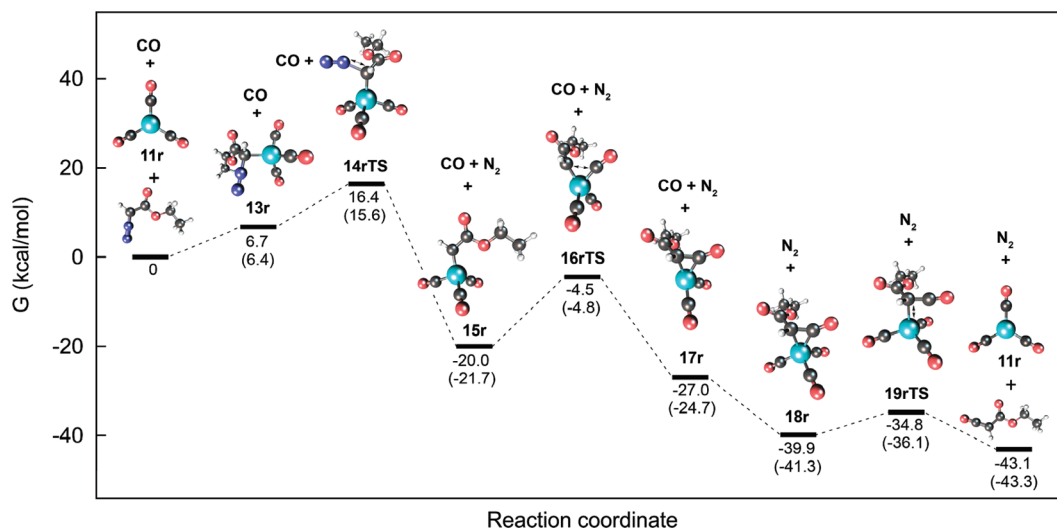
formation mechanism. The computed structures and the transition states obtained from **11** are depicted in Figure 10.

Figure 8. Computed structures of the transition state for intramolecular ketene formation **16rTS**, the coordinative unsaturated ketene complex **17r**, the coordinative saturated ketene complex **18r**, and the transition state for ketene dissociation **19rTS**. Bond distances are given in Å.

The transition-state structure for the  $\text{N}_2$  extrusion **14TS** shows some similarity to the radical **14rTS**, although the C–N bond as well as the Co–C<sub>carbonyl</sub> bonds are notably shorter in the former. The characteristic single imaginary frequency for **14TS** is  $527i \text{ cm}^{-1}$ . According to the IRC calculations the transition state **14TS** is connected with diazo complex **13**, which possesses  $\eta^2(\text{C}=\text{N})$  coordination. This kind of diazo coordination to transition metals is postulated,<sup>56</sup> but no example has been reported experimentally or theoretically, to the best of our knowledge. It must be noted, however, that the formation of **13** from **11** and EDA is endothermic by 10.3 kcal/mol (2.7 kcal/mol in the gas phase); therefore, both the free energy of activation (17.9 kcal/mol with solvation corrections and 12.6 kcal/mol in the gas phase) and the reaction free energy ( $-24.6$  kcal/mol with solvation corrections and  $-30.1$  kcal/mol in the gas phase) for the formation of the unsaturated carbene intermediate complex **15** are given with respect to **11** and EDA.

The connection of the carbene carbon to the neighboring carbonyl carbon via transition state **16TS** takes place with a smaller barrier compared to that for the pathway

(56) Dartiguenave, M.; Menu, M. J.; Deydier, E.; Dartiguenave, Y.; Siebald, H. *Coord. Chem. Rev.* **1998**, 178–180, 623–663.



**Figure 9.** Calculated free energy profile of (ethoxycarbonyl)ketene formation catalyzed by  $^*\text{Co}(\text{CO})_3$ .

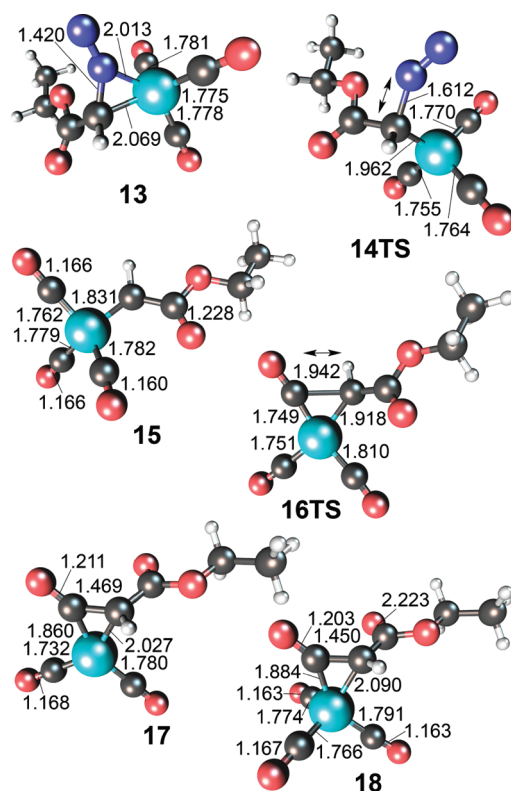


**Figure 10.** Computed structures of the diazo adduct **13**, the transition state **14TS**, the ionic carbene complex  $[\text{Co}(\text{CO})_3(\text{CHCOOEt})]^-$  (**15**), the transition state for intramolecular ketene formation **16TS**, the coordinative unsaturated ketene complex **17**, and the coordinative saturated ketene complex  $[\text{Co}(\text{CO})_3(\text{O}=\text{C}=\text{CHCOOEt})]^-$  (**18**). Selected bond distances are given in Å.

**15r**  $\rightarrow$  **16rTS**  $\rightarrow$  **17r**. The free energy of activation for this step is 8.5 kcal/mol (8.3 kcal/mol in the gas phase); the free energy of the reaction resulting in the coordinative unsaturated ketene complex **17** is  $-9.5$  kcal/mol ( $-9.0$  kcal/mol in gas phase). The characteristic single imaginary frequency for **16TS** is  $271\text{ i cm}^{-1}$ . Complex **17** takes up one external carbon monoxide to form the saturated ketene complex **18**.

The dissociation of (ethoxycarbonyl)ketene from **18** proceeds in a barrierless manner, providing tricarbonylcobaltate(−) (**11**) and closing the catalytic cycle. The free energy of the dissociation is 11.3 kcal/mol including solvation corrections and 18.1 kcal/mol in the gas phase.

The calculated free energy profile of the ketene formation reaction catalyzed by  $[\text{Co}(\text{CO})_3]^-$  is shown in Figure 11.

During the catalytic carbonylation of ethyl diazoacetate, we found a correlation between the decreasing  $\nu(\text{C}\equiv\text{O})$  intensity of  $[\text{Co}(\text{CO})_4]^-$  and the increasing intensity of a new  $\nu(\text{C}=\text{O})$  band at  $1637\text{ cm}^{-1}$  (see Figure 5). This new band might belong to an anionic species such as either  $[\text{Co}(\text{CO})_3(\text{CHCOOEt})]^-$  (**15**) or  $[\text{Co}(\text{CO})_3(\text{O}=\text{C}=\text{CHCOOEt})]^-$  (**18**), which are the anionic counterparts of **15r** and **18r**, respectively, and may be formed by taking one electron from  $[\text{Co}(\text{CO})_4]^-$ . Ketene formation via the anionic carbene intermediate cannot be excluded; the radical pathway seems to be more plausible. Calculations suggest for both pathways that the rate-determining step of the catalytic cycle is the activation of ethyl diazoacetate; thus, the  $\text{N}_2$  extrusion step results in the corresponding carbene complexes.

Mechanisms similar to those for the homogeneous cases can be assumed for the corresponding polystyrene-supported catalysts as well. On the supported catalysts, however, the site of the reaction is confined to the solvent-swollen polymer beads and restricted material transport may explain the much lower activities compared to those for the homogeneous cases. In accord with this assumption the turnover frequencies show no linear correlation with the initial concentration of ethyl diazoacetate above an initial EDA/catalyst molar ratio of 20 (see Table 3, entries 3–8). Under homogeneous reaction conditions complex **3** shows higher catalytic activity than either complex **1** or complex **5** (compare the TOF values of entries 1, 2, and 4 in Table 5). The order of activity is  $3 > 1 > 5$ . The polymer-bound analogues of **3** and **5** show the reverse order of activity under the same reaction conditions. A reason for the reverse order of activity is that the activation of the substrate occurs on the  $[\text{Co}(\text{CO})]_4$  part of the polymer-bound analogue of **5**, which is on the more accessible periphery of the catalyst beads, whereas the substrate activation in the case of the polymer-bound analogue of **3** occurs closer to the polymer core.



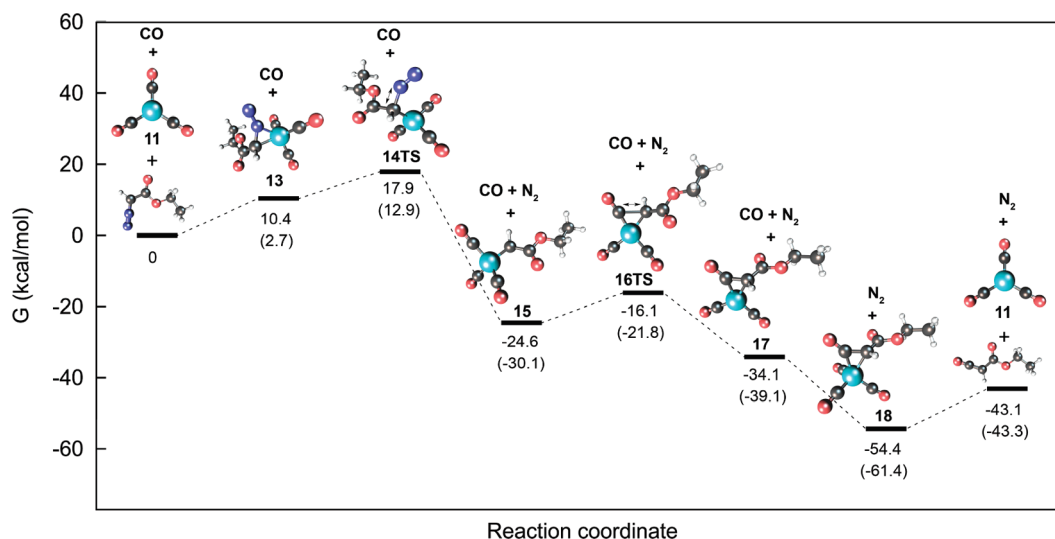


**Figure 11.** Calculated free energy profile of (ethoxycarbonyl)ketene formation catalyzed by  $[\text{Co}(\text{CO})_3]^-$ .

### 5. Conclusion

Modifying  $\text{Co}_2(\text{CO})_8$  and  $\text{Co}_2(\text{CO})_7(\text{CHCO}_2\text{Et})$  by  $\text{PPh}_3$  in the form of  $\text{Co}_2(\text{CO})_7(\text{PPh}_3)$ ,  $\text{Co}_2(\text{CO})_6(\text{CHCO}_2\text{Et})(\text{PPh}_3)$ , and  $[\text{Co}(\text{CO})_3(\text{PPh}_3)_2][\text{Co}(\text{CO})_4]$  results in catalysts with enhanced activity in the selective carbonylation of ethyl diazoacetate to (ethoxycarbonyl)ketene under ambient conditions. In the presence of ethanol the highly reactive (ethoxycarbonyl)ketene is trapped in situ and gives diethyl malonate as the final carbonylation product. Substituting  $\text{PPh}_3$  in  $\text{Co}_2(\text{CO})_7(\text{PPh}_3)$ ,  $\text{Co}_2(\text{CO})_6(\text{CHCO}_2\text{Et})(\text{PPh}_3)$ , and  $[\text{Co}(\text{CO})_3(\text{PPh}_3)_2][\text{Co}(\text{CO})_4]$  by polymer-bound  $\text{PPh}_3$  results in active and reusable catalysts for the selective carbonylation of ethyl diazoacetate in dichloromethane solution at  $40^\circ\text{C}$  and 11 bar pressure with up to 5.1 mol of product/(mol of catalyst) h turnover frequency.

**Acknowledgment.** We thank Profs. C. D. Hoff (Coral Gables) and G. Pályi (Modena) for stimulating discussions

and the Hungarian Scientific Research Fund for financial support under Grant No. OTKA NK 71906. We thank the Supercomputer Center of the National Information Infrastructure Development (NIIF) Program for support and the Flextra Lab KFT for access to the Bruker Tensor 27 FTIR spectrometer. T.K. acknowledges the support of a Bolyai Grant of the Hungarian Academy of Sciences and the support of the Research Team on Innovation (SROP-4.2.2/08/1/2008-2011) project. We thank the reviewers for their valuable suggestions.

**Supporting Information Available:** Figures giving solution IR spectra of the complexes **1** and **5–9**, solution and solid-state IR spectra of  $[\text{Co}(\text{CO})_2(\text{PPh}_3)]_x$ , and microscopic views of the PSDP-bound complexes and figures and CIF files giving X-ray structures and crystallographic data for complex **1** and  $\text{EtO}_2\text{CCH}_2\text{Co}(\text{CO})_3(\text{PPh}_3)$ . This material is available free of charge via the Internet at <http://pubs.acs.org>.